ABSTRACT

Title of Thesis: ENERGY TRANSPORT IN FIREFIGHTER PROTECTIVE CLOTHING

Kevin Spangler, Master of Science, 2008

Thesis directed by: Professor Marino di Marzo
Department of Fire Protection Engineering

Firefighting protective clothing is a highly advanced system designed to protect people from being burned in high temperature environments. Studies have shown a time delay from when a firefighter enters a high temperature environment until the skin feels a temperature increase. A similar time delay is found when the firefighter leaves the hot environment until the skin begins to cool.

An experiment was conducted that used thermocouples to observe room temperatures, outside gear temperatures and skin temperatures of firefighters in high intensity and long duration heat exposures. Computer models were created to duplicate and understand the resulting temperature response in the tests. A multi-layered model uses defined material properties to replicate the results and understand the contribution of the individual layers. The computer models can recreate the testing results and it is found that air gaps throughout firefighter gear are critical in providing protection from heat for the firefighters.

ENERGY TRANSPORT IN FIREFIGHTER PROTECTIVE CLOTHING

by

Kevin Spangler

Thesis submitted to the Faculty of the Graduate School of the
University of Maryland, College Park in partial fulfillment
of the requirements for the degree of
Master of Science
2008

Advisory Committee:

Professor Marino di Marzo, Chair
Professor Amr Baz
Professor Peter Sunderland

Acknowledgements

Appreciation is extended to Dr. Marino di Marzo, Chair of the Fire Protection Engineering department at the University of Maryland for heading this research and making this project possible. Also to Mr. Steve Edwards, Director of the Maryland Fire and Rescue Institute of the University of Maryland and Dr. Amr Baz, Professor of Mechanical Engineering at the University of Maryland for their involvement in the development and testing portions of this study. A special thanks to all the firefighters who participated in the live fire testing.

This study would not have been possible without the personal support of those closest to me. I would especially like to thank my brother for first introducing me to the fire service and always leading the way, my mother for her strength and guidance, my father for being a role model for all of us, and my fiancé for her continual confidence and encouragement.

TABLE OF CONTENTS

List of Tables

List of Figures

Chapter I: Introduction and Background

Firefighting is inherently dangerous and firefighters respond to thousands of unknown scenarios with random and intense conditions every day. These conditions include times of high intensity heat and the firefighters' lives depend on the protection provided by their personal protective equipment (PPE). PPE has advanced with technology but the development of a mathematical model with the ability to predict its performance is still of great interest. Studies have been completed in this area of interest with successful results compared to laboratory testing.

The National Institute of Standards and Technology (NIST) published a series of reports on understanding the performance of firefighter clothing. The goal was to create an accurate model for predicting the performance of firefighting gear. A model would be especially useful for a quick and cheap analysis of new fabric designs used for protective gear. One study [1] assumed that all the materials in the model were always dry and were below the temperature where thermal degradation occurred. Experimental data was collected from a three layer test sample of firefighting gear including an outer shell, moisture barrier and thermal barrier. The model was able to predict the interior layer temperatures within 5 °C, but the outer shell predictions were up to 24 °C higher than the experimental values.

A later study [2], also conducted by NIST, further investigated a mathematical model for predicting the thermal response of firefighter gear. The mathematical model created included transient heat and moisture transfer through multi-layered fabric assemblies, as

compared to only dry materials seen in the first study. Experimental data was collected from experiments performed in controlled laboratory settings on wet thermal liners subjected to radiative heat fluxes to study the heat and mass transport. The results from the mathematical simulations matched well with the experimental measurements. It is found that the moisture in the cloth vaporizes from the heat and recondenses in the interior of the cloth. It is observed that the amount of moisture within the layer significantly influences the temperature of the fabric layers and the total heat flux seen at the skin. The presence of this moisture can both enhance and reduce burn injury to the firefighter, depending on conditions. The testing concluded that moisture transport effects influence the heat and mass transfer across fabrics even at low intensity heat exposures.

Another report [3] in the NIST performance of firefighter clothing series includes testing for materials in high intensity, short duration heat exposures. Fabrics used for outer shell garments in firefighting gear were experimentally tested according to the standard Thermal Protective Performance (TPP) test. Mathematical models were found to agree within 6% of the experimental data for a single layer fabric under high intensity, short duration heat exposures. The calculation that best represented the results included equations that assumed 50% convective and 50% radiative heat transfer mechanisms. This study restricted simulations to single layers of protective fabric and suggestions are made for additional work on full firefighting turnout gear garments.

Lawson et al. [4] conducted research in 2005 to quantify the thermal properties of materials used in firefighting protective equipment. The thermal properties found in the study included thermal conductivity and specific heat along with the thermo-optical properties of absorptivity, reflectivity and transmissivity. The material thickness and densities were also recorded for the report. The specific heats were determined for temperatures between 0 °C and 100 °C and the thermal conductivity was found in a range of 20 °C to 100 °C. The maximum of 100 °C is determined as a temperature when material degradation does not occur and the ranges include temperatures when skin burns occur. The results from the study are particular useful in modeling of multi-layered systems for predicting the thermal transportation through firefighter gear.

Barry and Hill [5] created two and three dimensional computational fluid dynamic (CFD) models for predicting the performance of protective clothing. The models and simulations predict the protection and penetration of chemicals in military and emergency response personnel gear and thermal protection in steam or fire protective clothing. The simulation results shown in the report were focused on the chemical penetration of materials and air movement around a human object. One simulation showed the temperatures at skin level for a torso wearing a short sleeved shirt. Simulations for fully clothed fire protection gear were not completed and further information on the material properties are needed to advance to that level in CFD modeling. The report states accurate results with validation for moisture absorption, permeability and wicking, but additional testing data and simulations should be completed for additional applications.

Current Study

This report discusses two recent studies completed at the Maryland Fire and Rescue Institute (MFRI) in conjunction with the University of Maryland. This particular study uses heat transfer theory to create mathematical models to predict the skin temperature response of firefighters in extended heat exposures and compares the results to experimental data. Three models are created including two single layer assumptions and a multi-layer assumption. The multi-layer model uses specific material properties as obtained in previous studies to perform the calculation.

The experimental data for this study is different from previous studies in that it is obtained from full scale testing scenarios with firefighters being subjected to live fire. The data is representative of the protective clothing acting as an entire system, including the gear materials and additional clothing layers. The results further our understanding of conditions that firefighters experience and how the protective system works collectively as compared to standardized testing of small-scale samples in previous studies.

The objective of this study is to create a mathematical model that accurately describes the skin temperature response of firefighters seen in testing data for extended heat exposures. The study compares the accuracy of adiabatic and isothermal assumption models and observes the influence of individual layers in a multi-layer calculation. The testing data and theoretical models lead to an overall more complete understanding of the energy transport through firefighter protective clothing.

Chapter II: Experimental Testing

United States Fire Administration (USFA) reports show that from 1997 to 2004 between 91 and 112 firefighters die each year (plus 343 on 9/11). Of these deaths, an average of 10 firefighters per year die during training related incidences. Additional studies show that the leading cause of death for firefighters is cardiac arrest [7]. In 2005, the University of Maryland Center for Firefighter Safety Research and Development conducted a study resulting in the publication of Health and Safety Guidelines for Firefighter Training. The study was completed to fill the gap of limited research conducted on firefighters during training evolutions. The publication was created to provide guidelines for firefighter training in order to limit the number of injuries and deaths that occur each year.

The Center for Firefighter Safety Research and Development consists of three departments within the University of Maryland; Maryland Fire and Rescue Institute (MFRI), Fire Protection Engineering Department, and Small Smart System Center (SSSC). The Center's mission is to improve the safety of firefighters through the use of technology and the specialized talents of the participating departments.

The Maryland Fire and Rescue Institute (MFRI) is an internationally recognized emergency services training institute that conducts over 1,800 programs, training over 34,000 students each year. MFRI is frequently involved in research and development projects, especially those directly related to firefighter safety. The institute has state of

the art facilities including a three level obstruction maze and a structural firefighting building to use for live fire scenarios.

The Fire Protection Engineering Department at the University of Maryland is a national leader in fire protection engineering education and research. FPED regularly conducts research and experiments on fire related topics such as fire modeling, fire dynamics, smoke movement and burn injuries. The department provides an expertise at the technical engineering level for the Center's research.

The Small Smart System Center (SSSC) is within the A. James Clark School of Engineering at the University of Maryland. The department is dedicated to the advancement of research and education in the design, fabrication, and physics of smart systems. SSSC reaches many areas including virtual reality modeling, instrumentation and miniaturization. They provide an expertise in sensor development, data analysis and virtual firefighting to the Center's efforts. [8]

First Test

Two hundred firefighters participated in a study conducted at the Maryland Fire and Rescue Institute (MFRI). The firefighters were between 21 and 55 years of age, had a minimum of three years firefighting experience and held a Firefighter II certification as identified by the National Fire Protection Association (NFPA 1001, 1992). The testing occurred on twenty different dates between August 3, 2005 and October 14, 2005.

During the study, subjects wore the LifeShirt System, which was developed by VivoMetrics Government Services and is a highly innovative, multi-sensor, continuous monitoring system. For the purpose of the study, the LifeShirt System was able to monitor the subject's breathing (including tidal volume and respiratory rate) and accessory devices were added to monitor blood oxygen saturation (SaO_2), skin temperature and core body temperature. An electrocardiogram was recorded by three electrodes placed on the skin and an accelerometer was used to detect periods of rest versus periods of physical activity.

The subject's core body temperature was recorded with a CoreTemp^{TM} core body temperature monitoring system, which is an ingestible (pill-form) radio-transmitting thermometer. The signal was received by a monitoring system placed on the subject's hip and temperature readings were recorded. Subjects also provided a urine sample to find a urine specific gravity (USG) to be used as a baseline hydration status. A USG greater than 1.02 is considered to be euhydrated and USG less than 1.02 is considered to be dehydrated. Subjects also had their resting systolic and diastolic blood pressures taken as a baseline.

The burn room environment temperature was monitored at three different locations on both the first and third floors. At each of the locations a pole held in position six thermocouples, which provided the vertical temperature distribution at that location. Two flux gauges were also provided and installed by the National Institute of Standards

and Technology (NIST) in the third floor burn room. They were aimed horizontally at the fire and located at elevations of 0.3 and 1 meters above the floor.

The test subjects participated in two different training exercises, a maze evolution and burn evolutions. The maze evolution was held in MFRI's Breathing Apparatus Training Obstacle Course. This is a three level building which contains diminishing clearances, drop-offs, windows, crawl spaces, stairs and ladders [8]. The course is conducted in near darkness and the subjects completed it at their own pace. The LifeShirt System and accessory sensors recorded the subjects' physiological responses and temperatures throughout the course.

The live burn evolutions took place in MFRI's structural firefighting burn building. Each evolution consisted of two four-person hose teams and a Rapid Intervention Team (RIT). The evolutions were live burn scenarios that involved the two hose teams and the RIT as safety standby. The evolution started with a third floor fire involving one hose team and finished with a first floor fire involving a second hose team. Data was recorded for all three groups during the evolution.

The live burn evolutions started on the third floor of the building. The main fire was located in a small room with auxiliary fires burning in adjacent rooms to ensure limited visibility due to smoke. The first hose team pulled a 200 foot hose line, advanced to the second floor via an exterior stairwell, charged the line, and advanced to the third floor via an interior stairwell. Once staged on the third floor, the team advanced the hose line to

the burn room. The officer and nozzle person entered the burn room and positioned themselves approximately five feet and ten feet, respectively, from the fire [8]. The backup team member remained at the burn room doorway. After establishing their positions, all members maintained their positions for a period of four minutes to provide a period of heat exposure. After the four minutes of heat exposure, the team members extinguished the fire, exited the burn room and finally the burn building.

After the third-floor hose team exited the building, the first-floor hose evolution began. The first-floor hose team pulled a 150-foot hose line and entered the first floor of the building toward the burn room. After staging in an adjacent room, the team entered the burn room and immediately extinguished the fire. After extinction of the fire, backup persons performed a search and rescue operation within the burn room for a simulated victim (rescue manikin). Once the search was completed, the manikin was dragged from the building and the evolution finished when the last person from the first-floor hose team exited the door.

During the test evolutions, data was collected for environmental conditions and many physiological responses from the firefighters. For our particular study, the live burn room evolution data is of greatest importance, specifically the burn room temperatures, skin temperature, and response times. This data provides a basis for understanding the energy transport through firefighter protective gear.

The first floor evolutions showed rapid temperature digression with little sustained heat exposure to the fire. The rapid extinction of the fire occurred within one to two minutes of the firefighters entering the burn building, therefore having little impact on the environmental or firefighter thermal conditions. Figure 2.1 is a typical example of the temperature recordings and the short heat duration of the first floor evolutions.

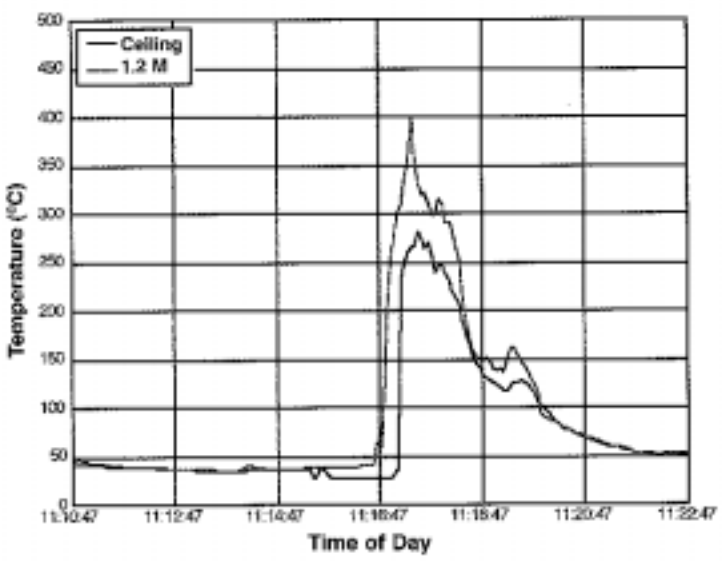

Figure 2.1 – Typical temperature profile for first floor evolutions [8]

The third floor evolutions provided the opportunity to collect data for firefighters under extended heat exposure events with high temperatures. This was possible because the subjects were asked to maintain their position for approximately four minutes before extinguishing the fire. Temperatures recorded by the thermocouples on the pole showed that the fire had enough time to produce a hot layer throughout the third floor. This hot layer is seen to be between 160-220 °C (320-430 °F) outside the burn room and an average ceiling temperature over 17 fires of 385 °C (725 °F) within the burn room.

Figure 2.2 is a typical example of the temperature profile data obtained for the third floor live burn test evolutions.

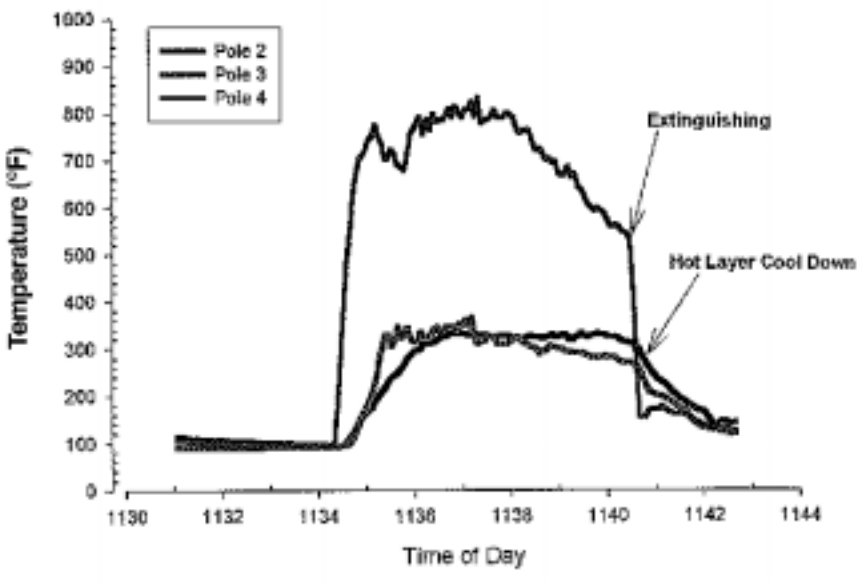

Figure 2.2 – Typical room temperature profile of third floor evolutions [8]

The skin temperature response for the third floor live burn evolutions were of greatest significance because of the extended heat exposure. The data consistently shows a delayed response of the skin temperature according to the external environment. The data allows us to determine an average time delay for when the skin first shows signs of the heat wave's penetration. This value is estimated at a temperature increase of 1 °C or 0.01 when normalized and is seen between 80 and 150 seconds. Figures 2.3 and 2.4 are examples of typical skin temperature responses from the third floor burn evolutions. It should be noted that the start time on the graphs is the time at which the subject first entered the hot environment.

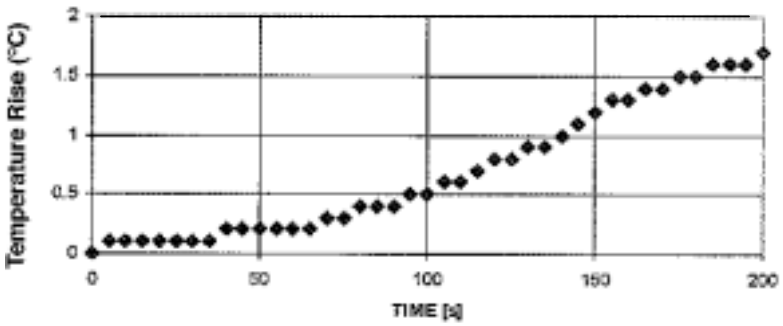

Figure 2.3 – Skin temperature response from third floor evolution [8]

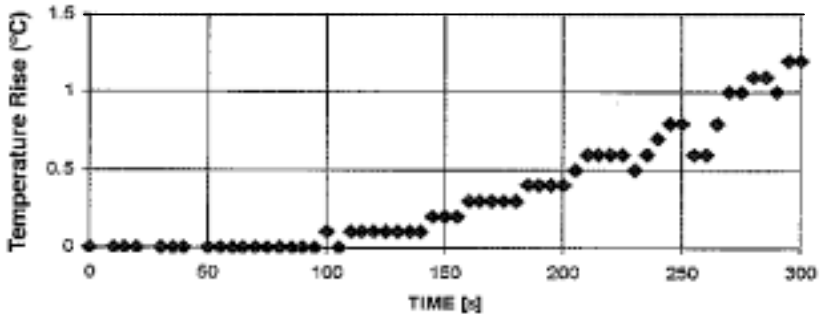

Figure 2.4 – Skin temperature response from third floor evolution [8]

Second Test

A second study was conducted to look at three additional areas as they relate to firefighter personal protective equipment (PPE). First is the recording of three temperatures; skin temperature, outer shell temperature and room temperature, and observing how they relate to each other. Second is the calibration of a predicted time until the skin is burned shown on the heads-up display (HUD) according to the subject's actual skin temperature. Third is the effect of varying PPE, including additional layers (t-shirt versus sweatshirt) and the weathering of gear (old gear versus new gear).

Thirty six firefighters participated in a second set of tests conducted at the Maryland Fire and Rescue Institute (MFRI). The firefighters were certified instructors according to NFPA and employed by MFRI. The testing occurred on three different dates in March 2007.

The firefighters were outfitted with two thermocouples each that connected to a portable data collection system worn on the subject's waist line. The portable data collecting system was also connected into the heads up display (HUD) located on the firefighter's SCBA regulator. The HUD is normally used for monitoring the air pressure in the SCBA cylinder, but was altered to display a predicted time until the firefighter is burned, which is calculated by the data collecting system. The portable data collecting system uses an algorithm to predict the future temperature felt by the firefighter at the skin's surface according to the time and intensity of heat to which he/she has been exposed. This device was battery operated and turned on by closing a circuit when connecting two wires located on the outside of the device.

The first thermocouple on the subject was located against the firefighter's skin at chest level and sewn on the inside of a cotton shirt which was worn throughout all test evolutions. This thermocouple was only used in recording the data of the firefighter's skin temperature. The second thermocouple was located on the lapel on the outside of the firefighter's gear, also at chest level. This thermocouple was used for recording the outside gear temperature and its data was also used to calculate the predicted skin temperature, which was displayed on the HUD. The thermocouple temperature data was

recorded on a memory card within the portable data collecting system, which was transferred to a computer after each evolution.

Currently, the HUD uses a series of five lights to display the air cylinder pressure, which is easily seen within the firefighter's field of vision. For this study, the HUD will be showing the predicted skin temperature from the data collecting device and start with all lights lit up, indicating no potential to burn. As the outside temperature rises and heat exposure time increases, the number of lights will start to diminish; first to 4 lights, then 3, then 2, then 1 and finally all five will start flashing as an intense warning to get to safety. Higher temperatures will cause the internal temperature to rise faster, and therefore the lights will diminish more quickly in these instances.

Throughout the test evolutions, multiple configurations of turnout gear and interior layers were used. This was to observe the contribution of additional layers to the transportation of heat and the effect of worn or well used gear. All subjects for all evolutions wore a cotton t-shirt that was provided by MFRI with the thermocouple sewn at the chest on the interior side as the innermost layer. The additional layers were altered to obtain data and show the effect of a sweatshirt versus no sweatshirt and old gear versus new gear. From the options, four possible configurations are created; 1. t-shirt, old gear 2. t-shirt, new gear 3. t-shirt, sweatshirt, old gear and 4. t-shirt, sweatshirt, new gear. A test matrix was created for the testing evolutions with subject number and turnout gear configuration.

The burn room was a small room (approximately 3.5 m x 3 m x 2.5 m) located on the third floor of MFRI's structural firefighting burn building. The fire consisted of three wooden pallets ignited by excelsior wood fibers against the back wall. Two fires were built so that the second fire could be ignited when the room temperature began to drop from the first fire extinguishing from burnout. The smaller room was used in order to easily regulate and ensure even temperature distribution.

A single pole located in the middle of the wall opposite the fires held in position six thermocouples, which were evenly spaced vertically. These thermocouples were used to measure the vertical room temperature distribution. The thermocouple wires were run down the exterior stairwell and into the command center located on the second floor. A real-time reading was visible on the computer monitor, which allowed for better temperature regulation of the fires from test to test.

Three subjects participated in each test evolution. Each subject was outfitted with a gear configuration different from the other two subjects for each evolution. The staging area, including the instrumentation and additional personnel, was located on the second floor directly below the burn room.

Once all subjects were fully dressed with turnout gear, helmet, SCBA and mask, the control instructors ignited the first fire on the third floor. The temperature readings from the thermocouple tree within the burn room were monitored to observe when the fire reached a quasi-steady state. This quasi-steady state occurred when the temperature

variation of each thermocouple was limited and the temperature of the third thermocouple from the ground (located at about chest level) gave a temperature reading between 400-500°F (200-260°C). Once this semi-steady state occurred, the test evolution time began.

During the evolutions, if the room temperature readings started to drop the second fire was ignited to bring the temperature back within the desired range. If the readings became too high, subjects were removed from the environment for their safety.

The three subjects were introduced to the burn room environment in two minute intervals with a minute of baseline temperature readings for each subject. At the start of the evolution (0 seconds), the first test subject's data collecting device was turned on by closing the circuit. The subject then had one minute to make his/her way up to the top of the stairs, just outside of the third floor burn room. A bell was sounded after one minute (60 seconds) to alert the subject of when to get into his or her predetermined test location. At the end of the second minute (120 seconds), the second test subject's data collecting device was activated. As with the first subject, he/she had one minute to go up the stairs. At the end of the third minute (180 seconds), the bell was sounded again to alert the second test subject to get into his/her designated position. Finally, the third test subject's data collecting device was initiated at four minutes and he/she entered into position at the sound of the bell at six minutes.

For the test evolutions, the subjects were positioned in the open doorways between the burn room and adjacent rooms. They were to be standing and at one arm's length away

from the door. The subjects were in the standing position because in previous tests when the firefighters were kneeling, the temperatures at the lower elevations were not high enough to obtain results. The subjects stood an arm's length away from the doorway so that they were affected by the temperature from the hot gasses that came out of the burn room, rather than the radiant heat from the fire at such a close distance.

Once in position, the subjects were asked to stand at the location until they felt that their skin temperature was at a point when a non-veteran firefighter should leave the area. During their time of heat exposure, the firefighter was also asked to observe what the lights on the HUD were doing/telling them to do.

When the subjects came out of the heat and down to the second floor (staging area), they were asked to stand and wait for an additional one to two minutes before removing any PPE, including the mask, helmet and coat. This was to allow the thermocouples to gather additional information for trends post heat exposure.

After removing their PPE, the data collecting device was turned off and removed from the gear. The memory card was removed and the temperature data from the evolution was downloaded onto a computer. The test subjects were then asked to write a few comments about how they felt and include how the lights of the HUD corresponded to their actual skin temperature.

The thermocouple data was compiled and compared to understand the variations between the different gear combinations. The written comments made by the subjects after each burn evolution were electronically transcribed and documented according to the burn evolution number and subject number, which referenced the gear configuration worn. The comments regarding the HUD response were used to correlate how well the data collecting system algorithm estimated the skin temperature according to the actual skin temperature felt by the subjects.

The thermocouple data was organized and included two temperature readings; the outside gear temperature and the corresponding internal skin temperature. The responses were normalized according to the peak temperature recorded by the outside gear thermocouple and was compiled onto four graphs, one for each gear configuration. The compiled data sets and graphs were compared against one another to observe the effect of each of the gear variations.

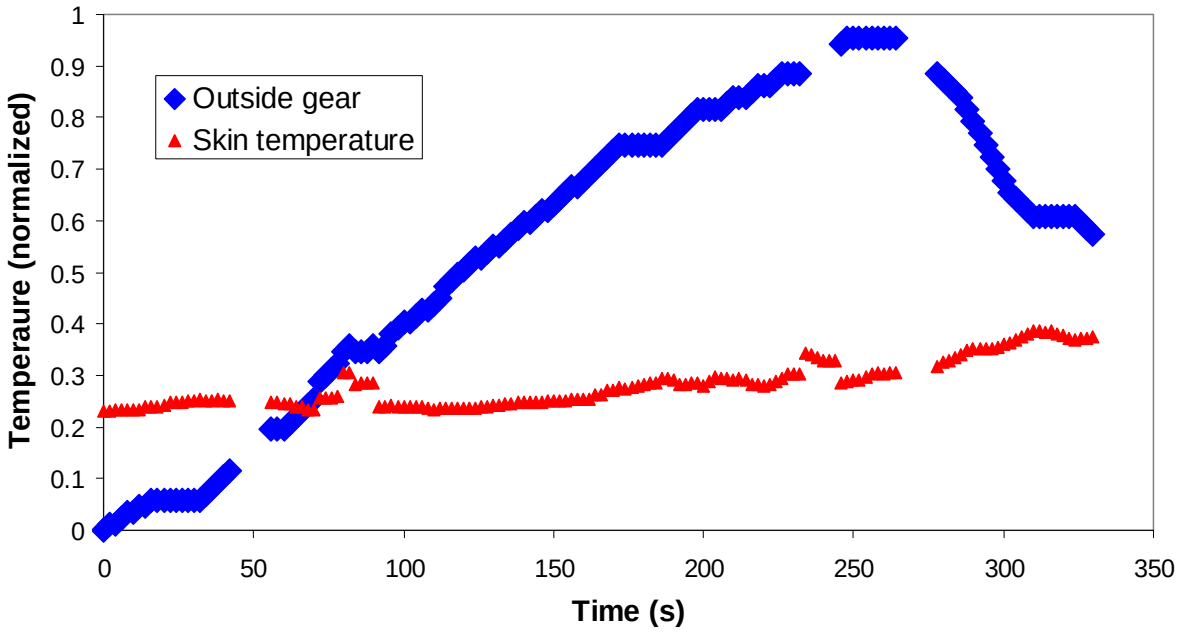

Figure 2.5 – Example of an outside gear temperature and skin temperature data set normalized to maximum outside gear temperature

The thermocouple data indicated a slower rise in temperature at the skin's surface for the old gear as compared to the new gear. However, the recorded exposure times showed that the subjects wearing the old gear left the burn room earlier than subjects wearing the new gear. The comments reported that the firefighters in the old gear left the burn room because of over exposure felt along the forearms and along the SCBA straps. The thermocouple data alone would indicate that the old gear performs better than the new gear, but the recorded exposure times and comments indicate that localized failures in the old gear make it less effective. The skin temperature thermocouple data are seen in Figures 2.6 and 2.7.

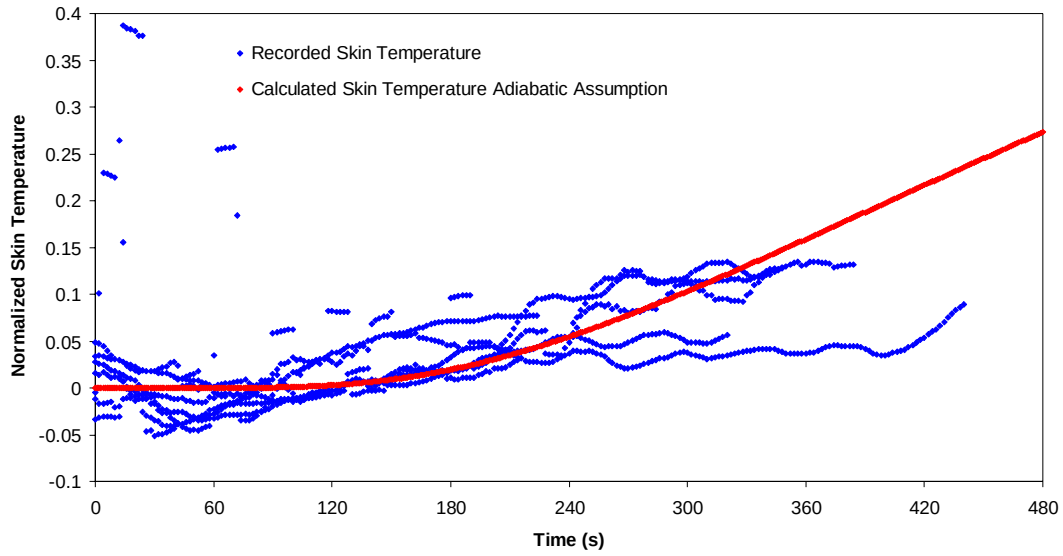

Figure 2.6 – Compiled skin temperature data for subjects wearing a t-shirt and new gear

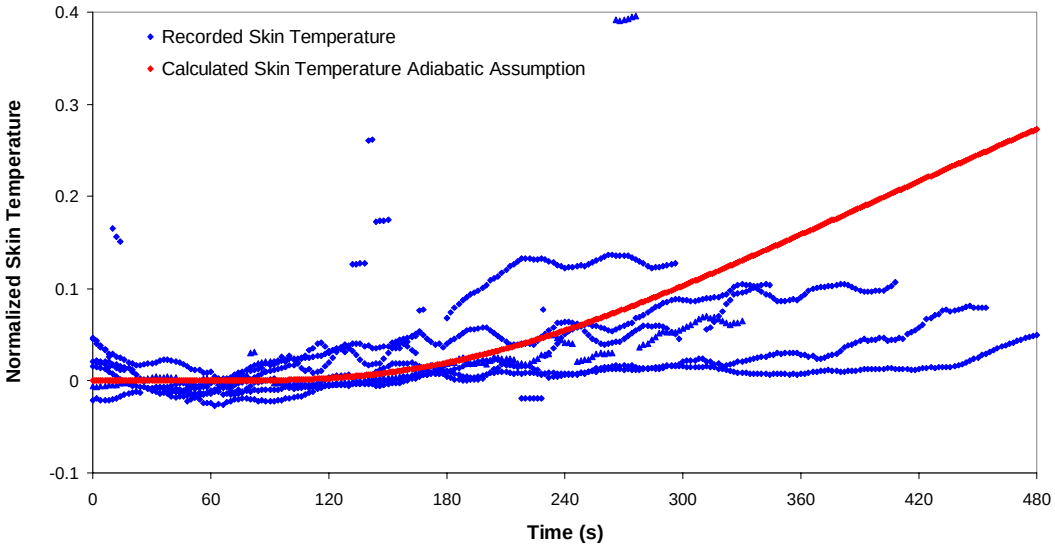

Figure 2.7 – Compiled skin temperature data for subjects wearing a t-shirt and old gear

The red line seen in the two graphs is a best fit line of the response when all t-shirt data is compiled. Using this line as a reference, it is seen that the new gear response is located very close to and above the line. For the old gear, it is seen that the temperature response

is more delayed with most of the data points staying below the line after the start of the temperature increase.

After closer observations of the gear, it is noticed that at the location of the thermocouples the old gear was more flexible and puffed out, creating a large air gap within the gear between the thermocouples. This large air gap was not present at the compressed location of the SCBA straps and was limited at the forearms. From this data, the specific contribution of the air gaps on the system is further examined.

As anticipated, the differences between the subjects who wore the sweatshirt versus those who did not favored the extra sweatshirt layer. The temperature at the skin's surface began to rise at a later time than for those who wore just a t-shirt. The slope of the temperature rise was also steeper, indicating faster temperature rise for the t-shirts versus a shallower slope of the temperature rise for the sweatshirt. This is especially evident in the extended length of time that the sweatshirt configurations stayed in the heat exposure. It is speculated that even though the sweatshirt provides more initial thermal protection that it will also retain more energy, therefore providing a longer increase in temperature even after leaving the heat exposure.

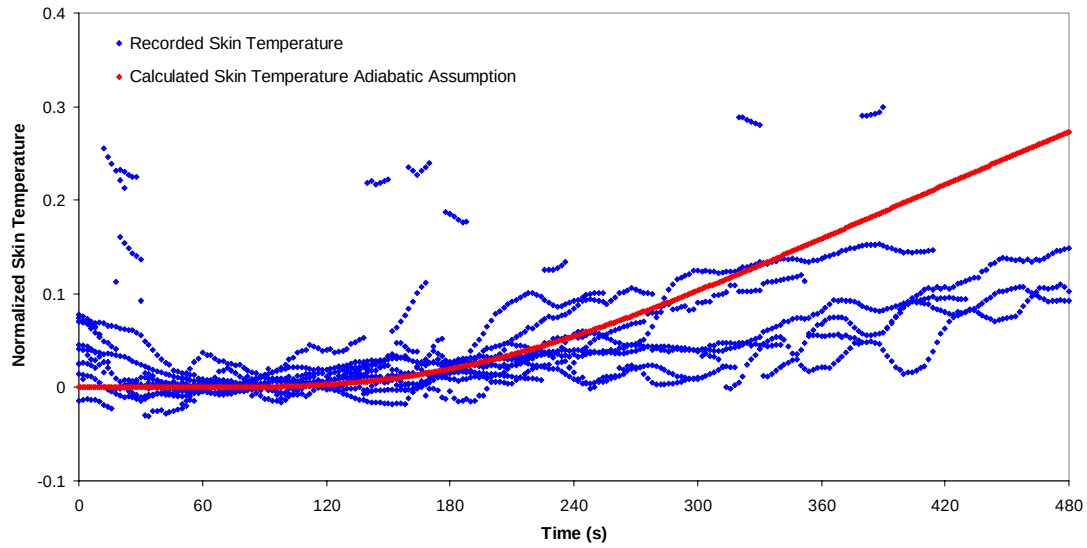

Figure 2.8 – Compiled sweatshirt skin temperature response for both old and new gear configurations

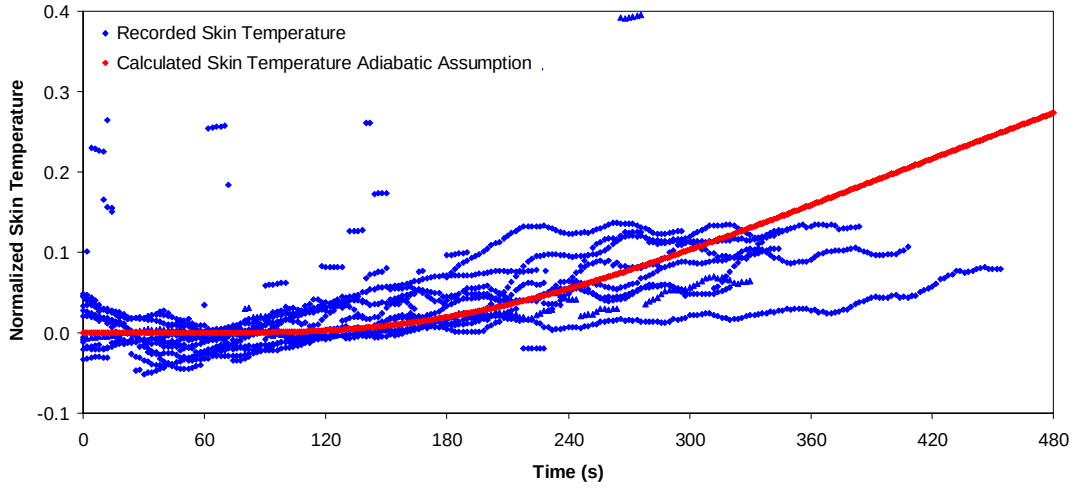

Figure 2.9 – Compiled t-shirt skin temperature response for both old and new gear configurations

The subjects' comments indicated that the temperature calculation seen on the HUD worked effectively, where the number of lights decreased as heat exposure time increased. The lights also degraded more quickly on the higher intensity fires than in the

lower intensity fires. Many subjects indicated that the lights' response may have been slightly fast, where the HUD indicated that they should leave the burn room when they felt that they were able to stay additional time. This observation indicates that the calibration of the algorithm and thermal diffusivity estimate for the gear may be too conservative and a more aggressive estimation should be made for more accurate results.

Material Properties and Measurements

NIST has conducted research on firefighter protective clothing materials as previously discussed. The results from the material property tests were of importance for this study when creating a multi-layered model for predicting the energy transport through the different layers. The materials' thermal conductivities, specific heats, densities and thicknesses were of specific interest. The material data from these reports that was used in this study can be seen in Appendix A.

Some properties for the t-shirts and sweatshirt, specifically the densities and thicknesses, were measured using instrumentation at the University of Maryland. Two different types of t-shirts were measured. One is a light-weight, 100% cotton undershirt and the other is a heavy weight, 100% cotton t-shirt, much like the ones used in the MFRI tests. Masses and volumes were obtained for each of the articles of clothing. The masses were found by using a calibrated digital scale from the Fire Engineering and Thermal Sciences laboratory (FETS lab) and recorded. The clothing volume was closely estimated with a volumetric container. One reading was taken with the clothing loosely placed in the

container and a second reading was taken with the clothing was under heavy compression. The two volume readings allowed for a calculation of a minimum and maximum density.

The thicknesses of the t-shirts and sweatshirt were found using a calibrated caliper and two flat metal plates. The metal plates were of known thickness and allowed for a larger surface area to minimize point compression by the caliper. Three measurements were taken for three different layer configurations. The first measurement was the thickness of the layer when there was little to no resistance on the material when it was moved between the plates. The second measurement was taken when there was some resistance to the material when slid back and fourth between the plates. The third measurement was taken under heavy compression when there was enough force on the layers that the material could barely move between the plates. These measurements gave maximum and minimum thickness, as well as an accurate midpoint estimate for thickness.

The three layer configurations included one layer, two layers and four layers of the same material. The three different measurements were taken for each configuration, giving a total of nine measurements per garment. The multiple layer measurements were taken to validate the thickness measurements and see if there was a doubling in thickness at each layer increase. The results from the measurements can be seen in Appendix A.

The thermal conductivity and specific heat of the t-shirts and sweatshirt were not measured in our lab. The values of these properties that were used for modeling purposes

were taken to be the same as those measured by NIST for cotton duck, a woven 100% cotton material. The confidence of these assumed values for modeling purposes is validated by the comparison of property values of similar materials with known values.

Chapter III: Theoretical Model

Initial Estimates

From the MFRI tests, the skin and burn room temperatures along with the recorded times enabled the formation of mathematical descriptions for properties related to the heat transfer through the firefighter protective gear. First a general value for the thermal diffusivity is found, which describes the gear's resistance to heat. A second parameter is a ratio of the thermal conductivity to the heat transfer coefficient, which describes how the material conducts heat according to the heat flux it encounters. These calculated values can then be used to calculate the heat transfer through the firefighting gear and be compared to the actual observed values.

An initial estimate of the thermal diffusivity of firefighter gear is found from the simplification of the heat transfer governing equation and data collected in the MFRI tests. The governing equation for the heat transfer through a semi-infinite solid is solved for a case of constant surface temperature. This boundary condition simplifies the equation to a temperature ratio equal to an error function. The temperature ratio value is a percentage of the overall temperature where there is evidence of the heat wave penetrating to our point of interest. For our scenario a temperature rise of 0.5% is chosen as a temperature increase with significance to the presence of the heat wave at the skin. From the recorded room temperature range of 180-240 °C (135-400 °F) and an initial temperature inside the gear of 37 °C (97 °F), the increase of 0.5 percent corresponds to a temperature rise of 0.7-1.0 °C. The derivation and simplification process is as follows:

Governing heat transfer equation;

$$\frac{\partial T}{\partial t} = \alpha \frac{\partial^2 T}{\partial x^2} \tag{3.1}$$

boundary conditions;

$T = T_{initial}$, *when* $x = 0$

$T = T_{surface}$, *when* $x = l$

$T = T_{initial}$, *when* $t = 0$

Therefore;

$$\frac{T - T_s}{T_i - T_s} = erf\left(\frac{x}{2\sqrt{\alpha t}}\right) \quad \Rightarrow \quad \frac{T - T_s}{T_s - T_i} = erfc\left(\frac{x}{2\sqrt{\alpha t}}\right) \tag{3.2}$$

since;

$$1 - \frac{T - T_s}{T_i - T_s} = \frac{T_i - T_s - T + T_s}{T_i - T_s} = \frac{T - T_s}{T_s - T_i} \tag{3.3}$$

and

$$1 - erf\left(\frac{x}{2\sqrt{\alpha t}}\right) = erfc\left(\frac{x}{2\sqrt{\alpha t}}\right) \tag{3.4}$$

Choosing a temperature percentage of 0.5%;

$$0.005 = erfc\left(\frac{x}{2\sqrt{\alpha t}}\right) \quad \Rightarrow \quad 0.995 = erf(2.0) \qquad [9] \tag{3.5}$$

Therefore;

$$\left(\frac{x}{2\sqrt{\alpha t}}\right) = 2.0 \quad \Rightarrow \quad x = 4\sqrt{\alpha t} \qquad [8] \tag{3.6}$$

where;

$x = gear\ thickness\ set\ at\ 10mm$

$t = time\ delay\ [s]$

$\alpha = gear\ thermal\ diffusivity\ [m^2 / s]$

With these values we obtain the following expression for thermal diffusivity of the gear:

$$\alpha = \frac{7E-6}{t} \qquad [8] \qquad (3.7)$$

The time delay in the expression above is the time from when the material is introduced to the heat exposure to when the point of interest observes an increase in temperature. This time is estimated at 150 seconds from the initial testing data. Using this time delay in the equation, an overall thermal diffusivity of 4.9 ± 1.2 E - 8 m^2/s for a 10 mm gear thickness is found [8].

A temperature rise at the skin is evaluated for high burn room temperatures and found to be on the order of 0.02 °C/s or 1.2 °C/min. Therefore, the time for the skin to reach 40 °C (104 °F) is 3 minutes and 20 seconds. Adding this time to the time delay for the gear and the time allowed in the burn room is on the order of five to six minutes before health risks associated with heat would occur. This estimated time is supported by the data from the MFRI tests, where the firefighters left the rooms when they felt unsafe, which corresponded to a time of five to seven minutes.

Another important parameter that can be considered from the temperature rise is the ratio of the gear thermal conductivity, k, and the heat transfer coefficient, h. This ratio allows us to describe the thermal conductivity of the overall gear system according to a heat transfer coefficient, which can be found from heat flux measurements. The correlation is derived from a governing equation from Incropera and DeWitt [9], based on surface convection and transient conduction with a semi infinite solid.

An expression describing t* can be found from the slopes and intersects of the lines from the graph of the mid-plane temperature in a slab.

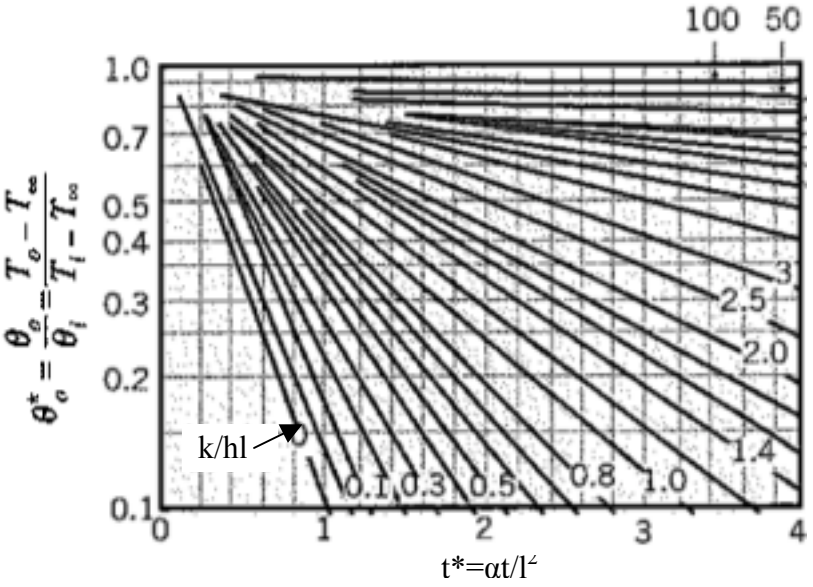

Figure 3.1 – Mid-plane temperature as a function of time in a plane wall [9]

The resulting relationship is described in the equation:

$$t^* = 7.0\frac{k}{hl} + 2.8 \tag{3.8}$$

An expression for the temperature difference is found and simplified as it relates to t*, thermal diffusivity, time and length.

$$\ln\left(\frac{T_\infty - T}{T_\infty - T_i}\right) = -\frac{3}{t^*}\frac{\alpha t}{l^2} = \ln\left(1 - \frac{\Delta T}{\Delta T_i}\right) \tag{3.9}$$

simplifying to;

$$\frac{\Delta T}{\Delta T_i} = 1 - e^{\left(-\frac{3\alpha}{t^* l^2}t\right)} \tag{3.10}$$

Rearranging the above equation and taking the derivative of the change in temperature according to time gives an expression for the slope of the line, S. This equation can be rearranged and simplified to an expression for k/h l. The equation simplification is made with the assumption that the internal conditions are approximately adiabatic because of the large difference of the low heat flux inside the gear compared to the high heat flux outside the gear.

$$S = \frac{d\Delta T}{dt} = \frac{3\Delta T_i \alpha}{t * l^2} \tag{3.11}$$

$$\Rightarrow \qquad S = \frac{3\Delta T_i \alpha}{\left(7.0\frac{k}{hl} + 2.8\right) l^2} \tag{3.12}$$

$$\Rightarrow \qquad 7.0\frac{k}{hl} + 2.8 = \frac{3\Delta T_i \alpha}{S\ l^2} \tag{3.13}$$

$$\Rightarrow \qquad \frac{k}{hl} = -\frac{2.8}{7.0} + \frac{3\Delta T_i \alpha}{7.0\ S\ l^2} \tag{3.14}$$

$$\Rightarrow \qquad \frac{k}{hl} = -0.4 + 0.429\frac{\Delta T_i \alpha}{S * l^2} \tag{3.15}$$

Where;

$$S^* = A \bullet S \tag{3.16}$$

and $A =$ *scaling value from graph*

For an assumed thickness of 10 mm, the expression can be written as:

$$\frac{k}{h} = (4E - 3) + (3E - 4)\frac{T_B - T_0}{S \cdot t} \qquad [8] \qquad (3.17)$$

where;

$T_B = temperature\ of\ \ burn\ room$

$T_0 = initial\ \ temperature\ inside\ \ gear$

$t = time\ \ delay$

A temperature difference of 150 °C is estimated and using 150 seconds for the time delay and 0.02 °C/s for the temperature rise, a k/h value of 0.02 is found. Heat flux measurements in the room were recorded between 7 - 11 kW/m^2, which correspond to an estimated transfer coefficient, h, of 60 W/m^2 K and therefore a gear thermal conductivity, k, of about 1 W/m K. The Health and Safety Guidelines for Firefighter Training report [8] states that this value for thermal conductivity for an insulating material seems high, but there is significant heat transfer from vapor generation and condensation, which could significantly affect this estimate.

A simplified model is created to calculate the temperature response at the skin according to an outside temperature with the calculated parameters from above. These calculated responses are then compared to the test evolution data for accuracy. The algorithm with inputs that best described the skin temperature responses was used for the data collecting system used in the second set of MFRI tests that was displayed on the HUD. The theoretical response can be seen in comparison with actual data below in Figure 3.2.

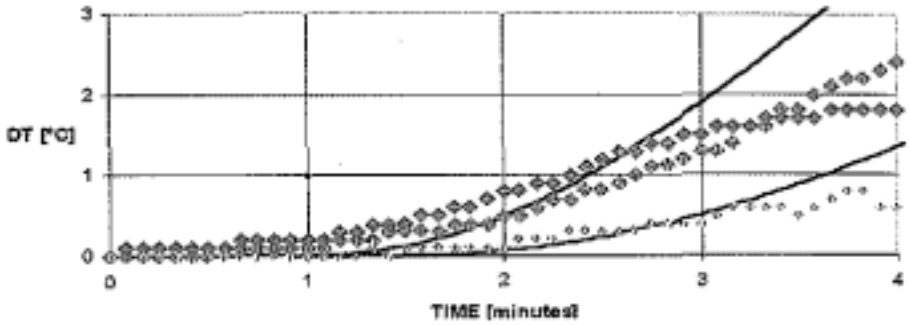

Figure 3.2 – Comparison of calculated response from simplified model and actual data [8]

Single Layer Assumption

A single layer assumption was created to further understand the results obtained from the MFRI tests. The theory is based on the linear flow of heat in a solid that is bounded by two parallel planes. The equations used were derived from the governing equation that was obtained from Carslaw and Jaeger's book *Conduction of Heat in Solids* [11].

The equation solves for a surface temperature, T, at a specified point, x, within the boundaries of the solid's length, l ($0 < x < l$). The end temperatures are fixed at $T_1=0$ and $T_2=1$, with an initial temperature of $T_0=0$.

Governing heat transfer equation;

$$\frac{\partial T}{\partial t} = \alpha \frac{\partial^2 T}{\partial x^2} \tag{3.18}$$

boundary conditions;

$T = T_1,$ *when* $x = 0$

$T = T_2,$ *when* $x = l$

$T = T_0,$ *when* $t = 0$

Therefore;

$$T = T_1 + (T_2 - T_1)\frac{x}{l} + \frac{2}{\pi}\sum_1^{\infty} \frac{T_2 \cos n\pi - T_1}{n} \sin \frac{n\pi x}{l} e^{-\alpha n^2 \pi^2 t / l^2} + \ldots$$

$$\ldots + \frac{2}{l}\sum_1^{\infty} \sin \frac{n\pi x}{l} e^{-\alpha n^2 \pi^2 t / l^2} \int_0^l f(x') \sin \frac{n\pi x'}{l} dx'$$

[11] (3.19)

recalling;

$T_1 = initial\ temperature = 0$

$T_2 = outside\ temperature = 1$

$f(x') = 0$

The equation simplifies to:

$$T = \frac{x}{l} + \frac{2}{\pi}\sum_1^{\infty} \frac{\cos n\pi}{n} \cdot \sin \frac{n\pi x}{l} e^{-\alpha n^2 \pi^2 t / l^2} \tag{3.20}$$

The point of interest for this study located at 3 mm of the length, representing the actual thickness of human skin as found in reports [12]. An initial estimated thickness for the firefighter gear is between 10 mm and 20 mm, giving an overall length (thickness) of the system between 13 and 23 mm. An alpha value for the calculation is such that the α / l^2 value is 4.9 E-4 s^{-1}, as estimated from the previous study and calculations.

An Excel spreadsheet is used to perform the single layer with fixed end temperatures calculation. The thermal diffusivity, α, point of interest, x, and total length, l, are set as variable inputs for simple calculation alterations. The coefficient and exponential terms are solved at increasing n values according to the factor inputs. The coefficient and exponent terms for each n value combine to solve the simplified equation at each time step. These calculated values for each time step are then summed to determine the skin temperature at each time step. An excerpt of the Excel file setup is seen in Table 3.1 and the resulting graph for skin temperature response versus time is seen in Figure 3.3.

Table 3.1 – Sectioned example of single layer assumption calculation

alpha	8.00E-08				
x	0.003	point of interest in m			
l	0.013	length in m			
n		1	2	3	4
coefficient		-0.66312	0.496354	-0.27433	0.059829
exponent		0.004672	0.018688	0.042048	0.074752
Time	Temp (v)				
0	0	-0.66312	0.496354	-0.27433	0.059829
1	0	-0.66003	0.487165	-0.26303	0.05552
2	-4.11001E-07	-0.65696	0.478145	-0.2522	0.051521

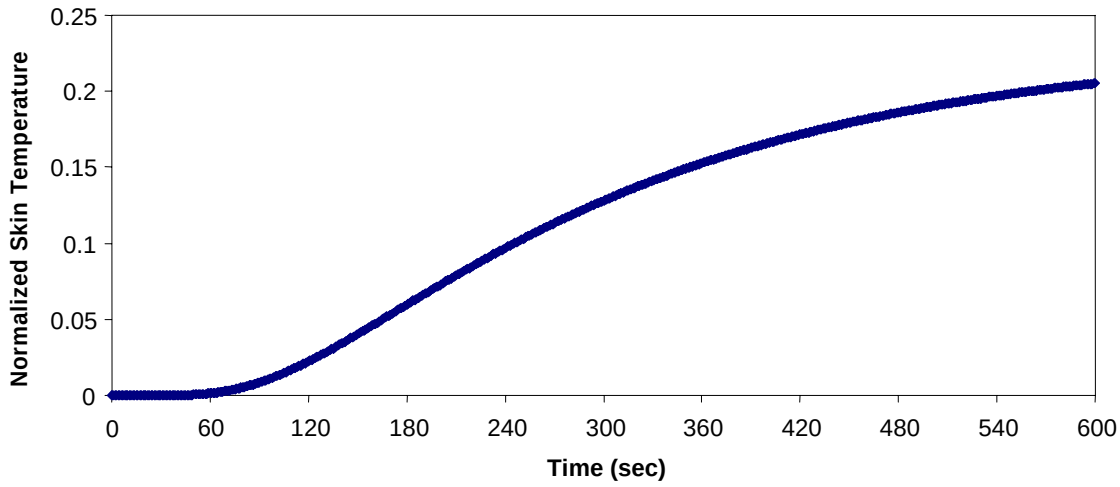

Figure 3.3 – Skin temperature output example of single layer assumption calculation

Multi-Layered Model

An analytical model was created using MATLAB to calculate the energy transport through a multi-layered system. This model is used to understand the contribution of each individual layer on the system's energy transfer as compared to previous studies where a single layer assumption was made. A tri-diagonal function solver was used to complete this calculation, which uses back substitution to solve a matrix form equation.

For the program, a couple mathematical assumptions were made for boundary conditions for the modes of heat transfer. The model assumes a constant core body temperature of the firefighter throughout the modeling time period. This assumption can be made because the realistic time and temperature values for observing gear performance do not exceed conditions that will affect the firefighters' core body temperature. Therefore,

throughout the calculation, the innermost point of the skin layer, node one, is kept constant at 37 °C (310 K).

The outside environment temperature is also assumed to be constant and the temperature of the point associated with the outside of the gear follows an exponential growth trend. This rise is patterned after the data recorded from the thermocouple positioned on the outside of the gear during the MFRI tests. The temperature of the thermocouple does not match the outside temperature because it was attached directly against the gear. When the subject was introduced to the heated environment, the gear acted as a heat sink and absorbed some of the energy. This caused a slower increase in temperature on the outside of the gear.

The equation for the ramping function uses the initial starting temperature and the specified maximum temperature along with a measured time constant to calculate the outside gear temperature. From the analyzed data, a time constant of 90 seconds ($1/t_c$=0.011 s^{-1}) is found for the heating response and 50 seconds ($1/t_c$=0.019 s^{-1}) for the cooling response. The calculated temperature values for the outside gear temperature are found from the following equation:

$$Temp_{outside\ gear} = T_i - (T_i - T_{\max}) \cdot \exp\left(-\frac{t}{t_c}\right) \tag{3.21}$$

where;

$T_i = initial\ temperature\ \ [K]$

$T_{\max} = maximum\ temperature\ \ [K]$

$t = time\ [s]$

$t_c = characteristic\ time\ [s]$

The assumptions allow for the following equation to be determined in which the multi-layered model solves using the tri-diagonal solver. The equation setup for the tri-diagonal function is further explained in a later section.

Governing heat transfer equation;

$$\frac{\partial T}{\partial t} = \alpha \frac{\partial^2 T}{\partial x^2} \tag{3.22}$$

boundary conditions;

$T = T_1 = 310K,$ *when* $x = 0$

$T = f(Temp_{outside\ gear}),$ *when* $x = l$

$T = T_0 = 300K,$ *when* $t = 0$

Giving;

$$T_n^N - T_n = \frac{1}{2}\left(\frac{\alpha \Delta t}{\Delta x^2}\right)\left(T_{n+1}^N - 2T_n^N + T_{n-1}^N + T_{n+1} - 2T_n + T_{n+1}\right) \tag{3.23}$$

where; $$F_o = \left(\frac{\alpha \Delta t}{\Delta x^2}\right) \tag{3.24}$$

Therefore;

$$-\frac{F_o}{2}\left(T_{n-1}^N\right) + \left(1 + F_o\right)T_n^N - \frac{F_o}{2}\left(T_{n+1}^N\right) = T_n + \frac{F_o}{2}\left(T_{n+1} - 2T_n + T_{n-1}\right) \tag{3.25}$$

The time constants for both heating and cooling were expected to be relatively constant. However, the data showed that the time constant for heating was higher than that for cooling. This means that a material that goes from a cool environment to a hot environment will take longer to match the surroundings than a material that goes from a hot environment to a cool environment. This phenomenon is mathematically investigated from the calculation of the heat transfer coefficient, h, for heating and cooling conditions.

As described earlier, the heat transfer coefficient is dependent on the temperature difference. It is anticipated that for a time of heating, there is a large h value because the temperature difference between the gear and the environment is very large. For cooling scenarios, the temperature difference is not as large, therefore having a smaller h value. The heating coefficient is calculated from the Nusselt and Rayleigh numbers, with properties seen below.

$$Nu_L = \frac{hL}{k} = C\ Ra_L^n \qquad [9] \qquad (3.26)$$

where;

$C = 0.1$

$n = 1/3$

$$Ra_L = Gr_L \cdot \Pr = \frac{g\beta(T_s - T_\infty)L^3}{\nu\alpha} \qquad [9] \qquad (3.27)$$

where;

$g = gravity = 9.81 m/s^2$

$\beta = 1/T \approx 1/300K$

$T_s - T_\infty = temperature\ change\ across\ air\ gap = \Delta T$

$L = width\ of\ air\ gap$

$\nu = kinematic\ viscosity$

$\alpha = thermal\ diffusivity$

Simplifying the expression;

$$\frac{hL}{k} = C\left(\frac{g\beta(T_s - T_\infty)L^3}{\nu\alpha}\right)^{1/3} \Rightarrow$$

$$\frac{h}{k} = C\left(\frac{g\beta(T_s - T_\infty)}{\nu\alpha}\right)^{1/3} \Rightarrow \quad \frac{h}{k} = C\left(\frac{g\beta(T_s - T_\infty)\rho^2}{\frac{\mu k}{c_p}}\right)^{1/3} \tag{3.28}$$

Resulting in the two values of;

$h_{heating}$

$$\frac{h}{k} = 0.1\left(\frac{(9.81 m/s^2)\left(\frac{1}{300K}\right)(200K)(0.852 kg/m^3)^2}{\frac{(2.3E-5\ m^2/s)(0.0346\ W/mK)}{(1016\ Ws/kgK)}}\right)^{1/3} = 183 \Rightarrow h_{heating} = 6.3\frac{W}{m^2\ K} \tag{3.29}$$

$h_{cooling}$

$$\frac{h}{k} = 0.1\left(\frac{(9.81 m/s^2)\left(\frac{1}{300K}\right)(50K)(0.7 kg/m^3)^2}{\frac{(2.6E-5\ m^2/s)(0.04 W/mK)}{(1030\ Ws/kgK)}}\right)^{1/3} = 93 \Rightarrow h_{cooling} = 3.7\frac{W}{m^2\ K} \tag{3.30}$$

This varying h value is significant in identifying the inverse Biot number, Bi^{-1}, which is used in describing the temperature change and slope in a plane wall, seen in Figure 3.4 below. In the semi-log graph, the inverse Biot number is compared against the temperature change for varying x/L values in a plane wall thickness. The point of interest

is related to the outside of the gear, therefore the x/L ratio is equal to 1.0. The inverse Biot number is defined by the equation below:

$$Bi^{-1} = \frac{k}{h\,L} \qquad [9] \qquad (3.31)$$

where;

$k = thermal\ \ conductivity$

$h = heat\ \ transfer\ \ coefficient$

$L = thickness$

From the equation, it is seen that a larger h value will produce a smaller Bi^{-1}. This smaller Bi^{-1} number corresponds to a smaller temperature difference correlation along the 1.0 ratio line in the graph below. Inversely, a smaller h value gives a larger Bi^{-1} and therefore larger temperature correlation. This temperature correlation is seen as the scaling factor, A, for describing the slope in equation 3.15 for determining k/h l, seen again below.

$$\frac{k}{hl} = -0.4 + 0.429\frac{\Delta T_i \alpha}{S^* l^2} \qquad (3.32)$$

Where;

$S^* = A \bullet S \qquad and \qquad A = scaling\ \ value\ \ from\ \ graph$

From the determined h values of 6.3 W/m^2 K and 3.7 W/m^2 K for heating and cooling, respectively, scaling factors of 0.85 and 0.87 are determined from the graph. This small difference is not a significant difference that describes the variation in the time constants for heating and cooling of the firefighting gear. These results do not support the initial

hypothesis that the varying density values and varying temperature differences alter the heat transfer coefficient enough to change the time constant for heating and cooling. Further mathematical investigations should be conducted in order to fully understand the heating and cooling differences seen in the firefighter gear.

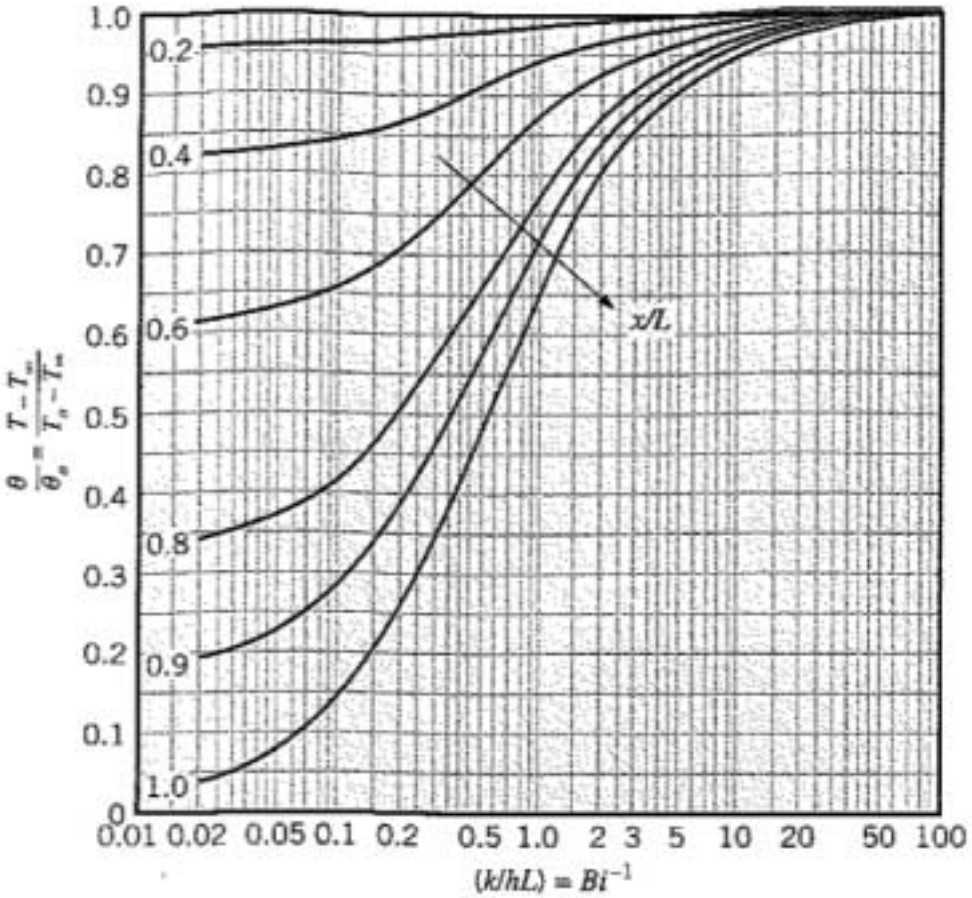

Figure 3.4 – Temperature distribution in a plane wall [9]

Another assumption for the multi-layered model is that the heat transfer method between and through all of the materials in the program is conduction. This includes the heat transport across the air gaps within the layers. Convection is not needed to be considered

in these layers because of the Rayleigh number correlation in external free convection flows. Incropera and DeWitt indicate that fluid motion is characterized by a recirculating or cellular flow for which fluid ascends along the hot wall and descends along the cold wall. For small Rayleigh numbers, $Ra_L \leq 10^3$, the buoyancy-driven flow is weak and heat transfer is primarily by conduction across the fluid [9]. The Rayleigh number is calculated for the air gaps in firefighting gear with property values seen below.

$$Ra_L = Gr_L \cdot \Pr = \frac{g\beta(T_s - T_\infty)L^3}{\nu\alpha} \qquad [9] \qquad (3.33)$$

where;

$g = gravity = 9.81 m/s^2$

$\beta = 1/T \approx 1/300K$

$T_s - T_\infty = temperature\ change\ across\ air\ gap = \Delta T$

$L = width\ of\ air\ gap \approx 0.004\,m$

$\nu = kinematic\ viscosity = 45.57x10^{-6}\ m^2/s$

$\alpha = thermal\ diffusivity = 66.7x10^{-6}\ m^2/s$

Therefore giving;

$$Ra_L = Gr_L \cdot \Pr = \frac{g\beta(T_s - T_\infty)L^3}{\nu\alpha} = \frac{(9.81m/s^2)\Delta T(0.004m)^3}{(300K)(45.57x10^{-6}m^2/s)(66.7x10^{-6}m^2/s)} = 6.88x10^{-25}\Delta T << 10^3 \qquad (3.34)$$

The calculated Rayleigh Number is orders of magnitude smaller than what is needed for buoyancy-driven flow. This indicates that the air gaps within the gear only need to consider conduction for heat transfer calculations.

The multi-layer program is intended to be user friendly so that the number and type of layers used in the system can be changed easily for different models. Additional inputs can be changed within the source code. These include; dx, dt, temperature in heated environment, temperature out of heated environment, run time of model and modeled exit time from heated environment.

When the program is run, the user is asked to specify inputs. The program first asks for the number of layers for the specific system. This includes skin, all materials and air gaps. The next step is to specify each layer, which is designated by a number and is given to the user in the form of a list. The layers are chosen with skin as the first layer and then in sequential order from the innermost to outermost layer. By altering the source code, the outside environmental temperature can also be asked as an input, along with the total time of simulation and the exit time from the heated environment.

The program uses the layer input numbers and references data from a created material property list. This list includes the thickness, density, thermal conductivity and specific heat of materials worn by firefighters along with properties of air, water and human skin. The material thicknesses are used to define the number of points or nodes through each layer according to the specified dx value. The thermal conductivity, specific heat and density values are used along with the dx and dt values to find the dimensionless Fourier number, F_0. The Fourier number is defined as:

$$F_O = \frac{\alpha t}{l^2} \tag{3.35}$$

where;

$\alpha = thermal\ diffusivity\ [m^2 / s]$

$t = characteristic\ time\ [s]$

$l = length\ through\ which\ conduction\ occurs\ [m]$

And the thermal diffusivity is defined as:

$$\alpha = \frac{k}{\rho Cp} \tag{3.36}$$

where;

$k = thermal\ conductivity\ [W / m K]$

$\rho = density\ [kg / m^3]$

$Cp = specific\ heat\ [J / Kg\ K]$

Because of changing material properties, the thermal diffusivity value and consequently the F_0 number changes from node to node. The nodes completely within a layer can be calculated with a straight calculation using the given material properties. However, the nodes that are caught between layers offer potential complications from varying material properties, as depicted in the diagram below. These in-between nodes will share properties from the two adjoining layers. Therefore, the thermal diffusivity value is calculated by the individual thermal conductivity values, k, and an averaged density and specific heat value from the two adjoining layers, lumped together as a single value, $\overline{\rho c}_p$, and calculated as:

$$\overline{\rho c}_p = \frac{\rho_1 c_{p1} + \rho_2 c_{p2}}{2} \tag{3.37}$$

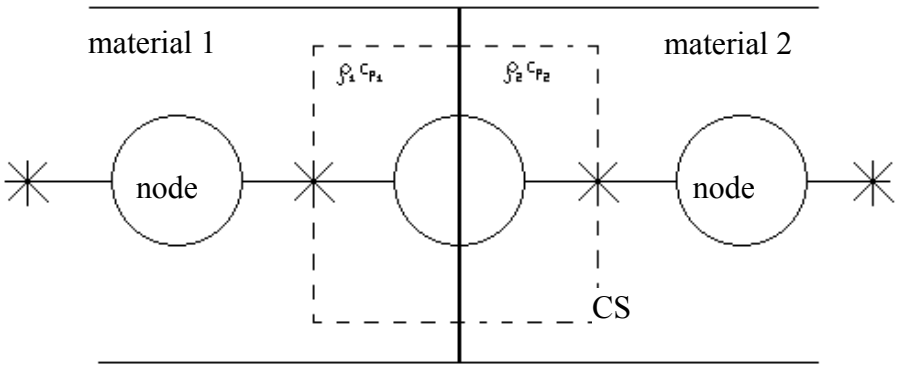

Figure 3.5 – Control surface and influential properties for a node located between two material layers

The calculated F_0 numbers are put into a matrix form equation according to their layer position and used in the tri-diagonal calculation. The tri-diagonal solving function uses the matrix of F_0 numbers and a corresponding single column matrix of initial temperatures, T_o, as inputs and solves for a new matrix of temperatures, T_n. The calculation uses back substitution and solves for these new temperatures. Additional iterations are completed according to the specified time step, dt, by substituting the previously calculated temperature array, T_n, into the initial temperature matrix, T_o. This matrix is used along with the F_0 number matrix to calculate another set of new temperatures. The matrix setup and temperature substitution is seen below:

$For\ t = 0,\ T_O = 310\,K$

$$\begin{bmatrix} 1 & & & & \\ -\frac{F_o}{2} & 1+F_o & -\frac{F_o}{2} & & \\ & -\frac{F_o}{2} & 1+F_o & -\frac{F_o}{2} & \\ & & -\frac{F_o}{2} & 1+F_o & -\frac{F_o}{2} \\ & & & & 1 \end{bmatrix} \begin{bmatrix} T_{N1} \\ T_{N2} \\ T_{N3} \\ T_{N4} \\ T_{N5} \end{bmatrix} = \begin{bmatrix} T_{O1} \\ T_{O2} \\ T_{O3} \\ T_{O4} \\ T_{O5} \end{bmatrix} \tag{3.38}$$

$For\ t = 1,\ T_O = T_N$

$$\begin{bmatrix} 1 & & & & \\ -\frac{F_o}{2} & 1+F_o & -\frac{F_o}{2} & & \\ & -\frac{F_o}{2} & 1+F_o & -\frac{F_o}{2} & \\ & & -\frac{F_o}{2} & 1+F_o & -\frac{F_o}{2} \\ & & & & 1 \end{bmatrix} \begin{bmatrix} T_{N1} \\ T_{N2} \\ T_{N3} \\ T_{N4} \\ T_{N5} \end{bmatrix} = \begin{bmatrix} T_{O1} \\ T_{O2} \\ T_{O3} \\ T_{O4} \\ T_{O5} \end{bmatrix} \tag{3.39}$$

The use of the tri-diagonal function was validated through a series of programs. These programs started with basic principals whose results were compared against known growth function results.

The initial program created is a slight variation of the single layer assumption equation from *Conduction of Heat in Solids* by Carslaw and Jaeger [11] seen in the previous section. This single layered insulated solid has a normalized temperature and normalized thickness. The interior temperature (T_1) is fixed at 0, the exterior temperature (T_2) is fixed at 1 and the slab thickness is from 0 to 1. The governing equation is and simplified to observe a point located halfway through the thickness.

$$Temp = \frac{2}{l}\sum_{1}^{\infty} e^{-\alpha n^2\pi^2 t/l^2}\sin\left(\frac{n\pi x}{l}\right)\left[\int_0^l f(x)\sin\left(\frac{n\pi x'}{l}\right)dx' + \ldots + \frac{n\alpha\pi}{l}\int_0^t e^{-\alpha n^2\pi^2\lambda/l^2}\left\{\phi_1(\lambda) - (-1)^n\phi_2(\lambda)\right\}d\lambda\right]$$

[11] (3.40)

The equation simplifies to the following for a point of 0.5:

$$Temp = \sum_{1}^{\infty}\frac{\sin\left(\frac{\pi\cdot n}{2}\right)}{\left(\frac{\pi\cdot n}{2}\right)}\left(1-\exp\left(-\frac{\alpha\cdot n^2\pi^2}{l^2}t\right)\right) \quad (3.41)$$

Because of the normalized conditions of the boundary conditions, the temperature at a thickness position of 0.5 will asymptote to a normalized temperature of 0.5 as seen in Figure 3.6. This is because the final temperature distribution throughout the thickness is a straight line between 0 and 1. This program's results are of know accuracy and are used as a baseline for validation of the tri-diagonal function and the multi-layered problem.

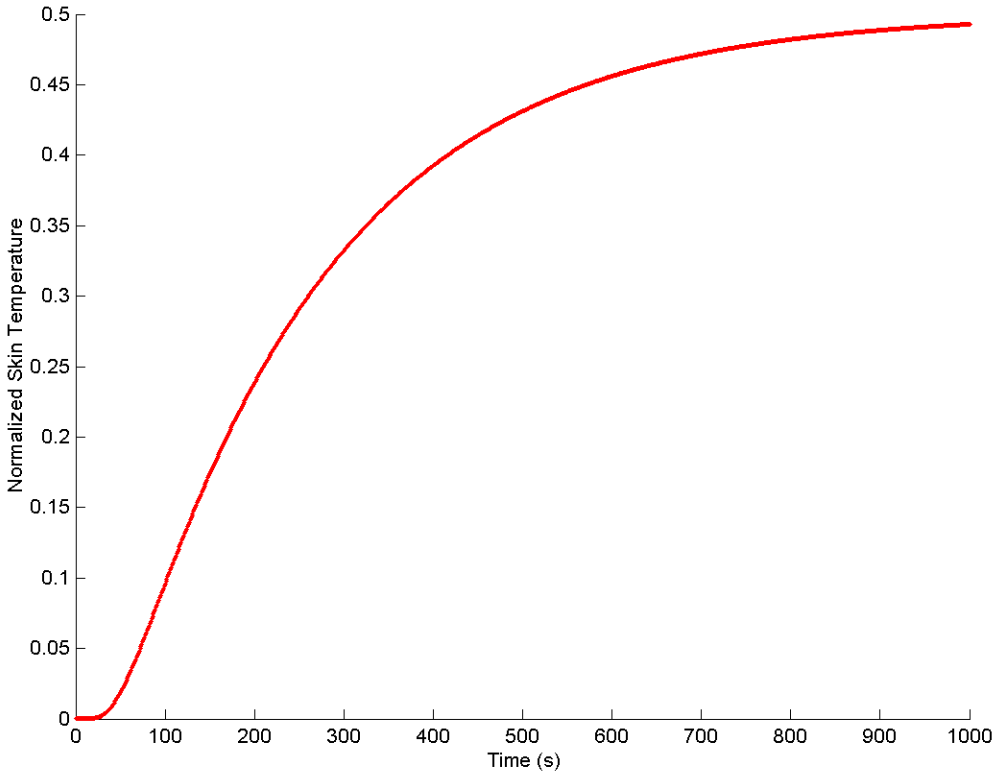

Figure 3.6 – Temperature of point x=0.5/1.0 asymptoting to temperature of 0.5

A second program is created with the same alpha value and normalized thickness and temperatures as the first program, except that it uses the tri-diagonal solving file for the calculation. Producing the same temperature output curve for a location of 0.5 validates the use of the tri-diagonal function. The program also uses a calling function that references the property list of materials. When the program is run, the user identifies the alpha value, which should be the same as the previous program, and the number of layers to be used for the calculation. Because this program uses an input alpha value, only the thicknesses of the materials are used from the property list. Therefore, an extra material

is created that has a specified thickness of 0.5, and two layers of this material are used to create a thickness of 1.

The results from the second program match those obtained in the first program. These results confirm the use of the tri-diagonal function as an accurate calculation method for the multi-layered system. The resulting graph from the second program is compared to the first program's results in Figure 3.7.

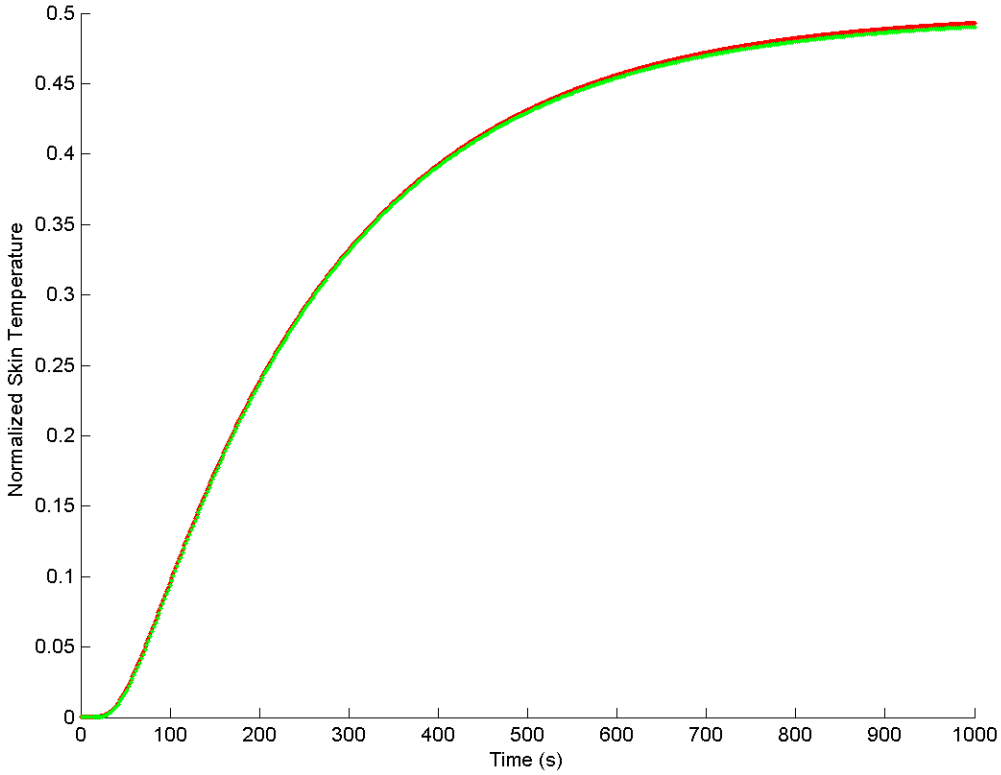

Figure 3.7 – Tri-diagonal function validation against simplified model

A third program is created which uses a ramping function for the outside temperature, instead of an instantaneous temperature rise. This ramping function is created from the

data of the outside gear temperature from the second set of MFRI tests and discussed earlier. The program looks at the middle location of the overall thickness and will still asymptote to 0.5. However, because of the delay from the ramping function, the temperature of the point of interest will reach its maximum at a later time. This program is intended to show that effect of that temperature delay from the ramping function.

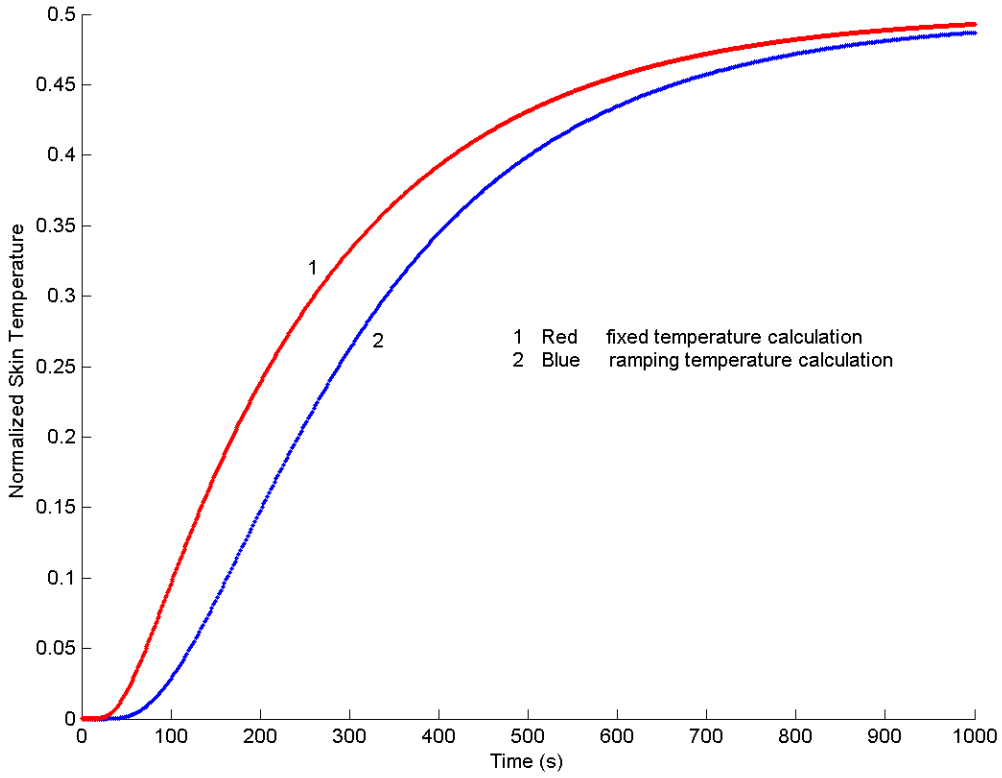

Figure 3.8 – Ramping temperature model results compared against fixed temperature model

A fourth and final program is created which observes the temperature at the position of the skin surface of 3 mm, but still has an input alpha value. This program calculates the actual alpha value of the skin from its properties, but uses the input alpha value for the

other layers. This program is intended to be used to correlate a multi-layered system with varying alpha values to a single layer system with a single alpha value. This program's results should be used and compared to the final multi-layered program's results and is discussed in a later section.

Chapter IV: Results

The purpose of this study is to gain a more complete understanding of the energy transport through firefighter gear from testing data and theoretical modeling. The three calculation methods in this study include; a single layer assumption with fixed temperature conditions, a single layer assumption with one fixed temperature and one ramping temperature, and a multi-layered assumption model. Each model calculates the energy transport and solves for the skin temperature according to specific boundary conditions. The results for the calculated skin temperature in each are compared against one another and to the temperature rise seen in the testing data to determine the accuracies of the models.

Between the two MFRI tests, the data shows an overall time delay in the temperature response at the skin's surface between 80 and 150 seconds. The time delay is the time from when a subject is first introduced to a heat exposure until the skin temperature observes an increase in temperature. Because of the thermocouples' margin of error and fluctuating temperatures, the time delay is determined as the time until the temperature shows a steady increase above a value of 0.01 of the normalized temperature. Figure 4.1 is a result from the first set of MFRI tests, with a time delay of 100 seconds. Figures 4.2 and 4.3 are examples from the second set of MFRI tests with time delays of 140 and 95 seconds respectively.

After the time delay, the temperature rises at a steady rate reaching an estimated normalized temperature of 0.1 between 300 and 350 seconds. This benchmark

temperature is an averaged value estimated across all the gear configurations from the second tests. The exact time delay and time to reach the 0.1 temperature varies according to the number of layers and the condition of the gear. A compiled data set including results from t-shirt, sweatshirt, old gear and new gear can be seen with a curve fit in Figure 4.4. Note that time = 0 for all graphs is when the subject entered the burn room.

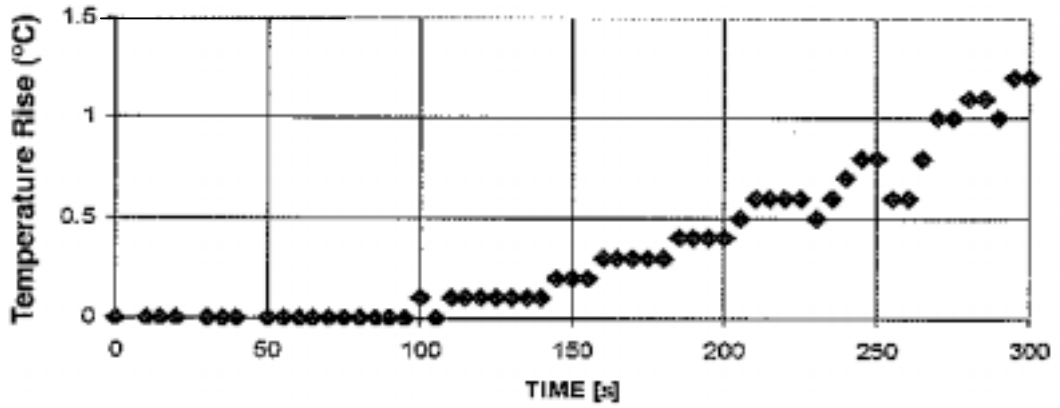

Figure 4.1 - Skin temperature rise example with time delay of 100 seconds [8]

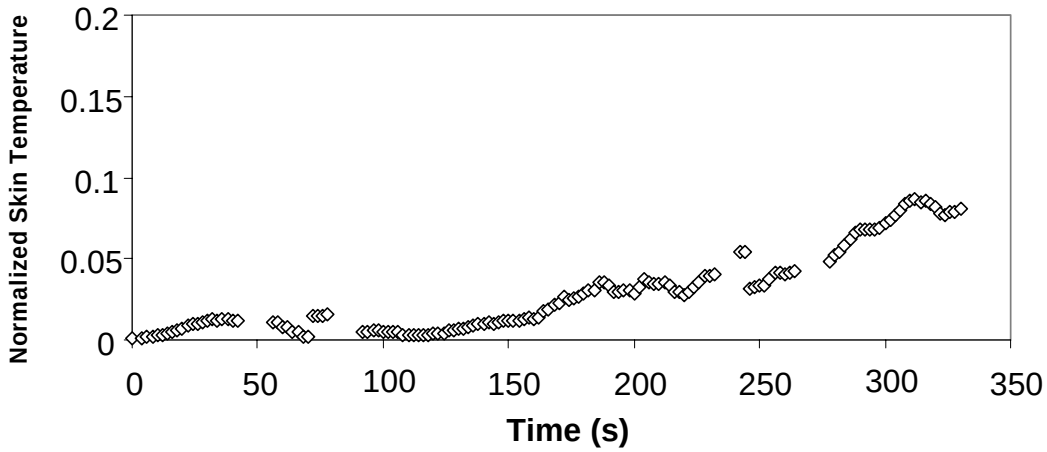

Figure 4.2 – Skin temperature rise example with time delay of 140 seconds

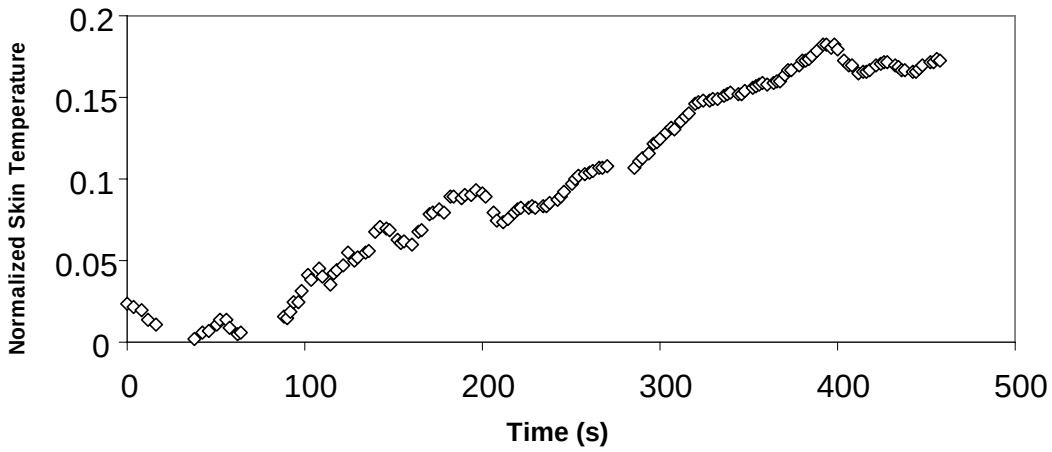

Figure 4.3 – Skin temperature rise example with time delay of 95 seconds

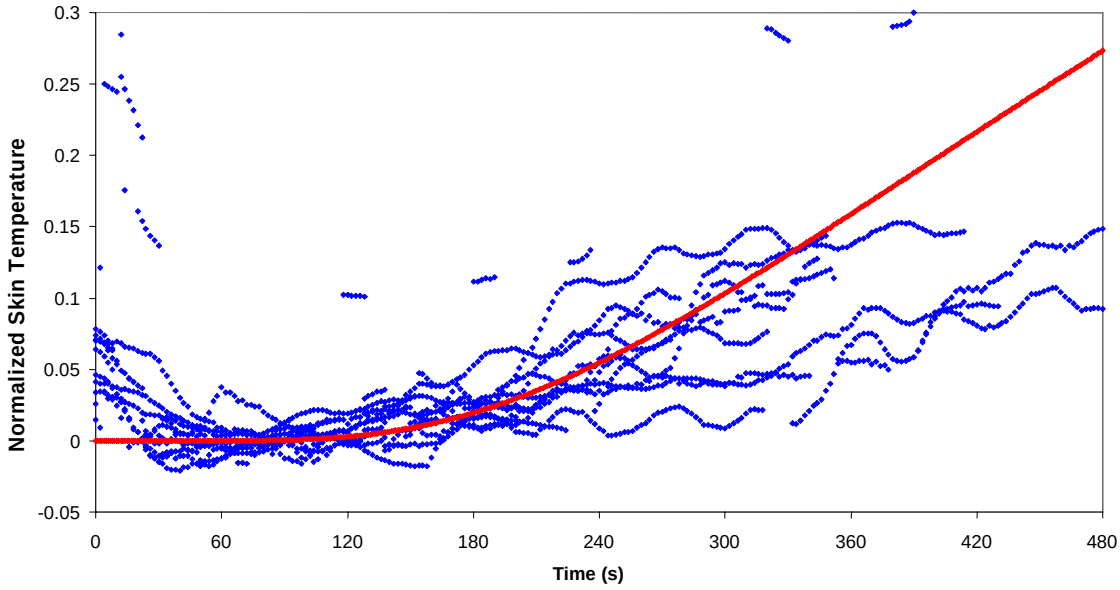

Figure 4.4 – Compiled skin temperature response data with fit curve

The curve fit seen in the graph above was calculated using an Excel spreadsheet. The calculation uses a ramping function for the outside gear temperature with an estimated time constant of $1/t_c$=0.015 s^{-1}, a thermal diffusivity of 5.5E-8 m^2/s and a thickness of 10

mm. This correlates to an α / l^2 value of 5.5E-4 s^{-1}. The calculation is an adiabatic consideration, such that there is a zero flux condition at the skin's surface. The calculated values of the curve's response are seen as an average representation of all the data collected and responds according to the time delay and time to reach 0.1 as discussed above. This calculation was used in the programming of the data collecting device which calculated the time until burn seen in the HUD during the tests. This representative curve is used as the temperature response when comparing the calculated results of other programs.

The test results and best curve fit are recreated by the three different calculation models. The two single layer assumption models calculate the response with defined thickness and thermal diffusivity values. The values that reproduce the results are then compared to the values that were theoretically calculated and previously discussed. The multi-layer model uses material values for various layers to calculate the temperature response. This solution is also compared to the single layer assumption to understand if there is a correlation between the two models.

The best fit curve seen in the graphs below for the comparison of the models is calculated for a strictly heating system, without cooling. This means that the best fit graph converges to a temperature of 1 at $t=\infty$. This comparison is made because all models are calculated such that the heat exposure is constant for 600 seconds and cooling does not occur. Most of the data collected in the tests is seen to peak between 0.15 and 0.2 and does not exceed 480 seconds, and this range is most important for model's accuracy to

the testing data. However, the constant heating comparison in the best fit model, which extends longer and hotter than the testing data, is important in that it can help determine the limitations of the other model calculations.

For the modeling purposes, an estimate of the overall protective gear thickness needs to be determined. The actual structure and fit of the firefighting gear is bulky, creating a thick system from air trapped within the layers. Measurements were taken to find the actual thickness of firefighting gear when worn by a person. Two firefighters, both of average build, volunteered for personal measurements with their own standard turn-out gear coat. Twelve circumference measurements were taken between four different locations on each of the subjects including; forearm, bicep, chest and stomach.

The first measurement at each location was on bare skin to give a base reading. The second measurement was with gear being worn and the measuring tape cinched tight around the location. This gave an estimated compressed thickness. The final measurement at each location was with the gear on and the measuring tape wrapped around the gear without compressing it. This gave a maximum gear thickness.

The measurements were considered to be circumferences of a cylinder, which allowed for the calculation of diameters at each measuring point. Subtracting the body diameter from the gear diameter and dividing by two led to the estimated gear thickness for compressed and relaxed situations on a firefighter. The results at each location were averaged between the firefighters and then all of the results were averaged together for a final

average gear thickness. The measurements were consistent for all areas, with a final average compressed thickness of 20 mm and a final average uncompressed thickness of 40mm. The sum of the material thicknesses is on the order of 7 mm to 10 mm, indicating that air gaps make up 10 mm to 30 mm of the overall thickness. Because of the location of the thermocouples during the full scale tests, it is assumed that a gear thickness of 40 mm is more closely associated with these results. The full set of gear thickness measurements and results can be seen in Appendix A.

Single Layer Assumption with Fixed Temperatures

The first calculation is performed using Excel with the equation and setup previously described and is a single layer assumption. For this model, the temperature (T) is fixed at both endpoints and normalized such that at x = 0, T = 0 and at x = l , T = 1. The gear thickness is set at 20 mm and 40 mm for two different models, with a skin thickness of 3 mm. The resulting graph is seen in Figure 4.5. The thermal diffusivity value is set such that the results produce a time delay between 80 and 150 seconds and a temperature rises to a point of 0.1 between 300 and 350 seconds. The values for the time at the temperature locations of 0.01 and 0.1 were found from the output data of the spreadsheet.

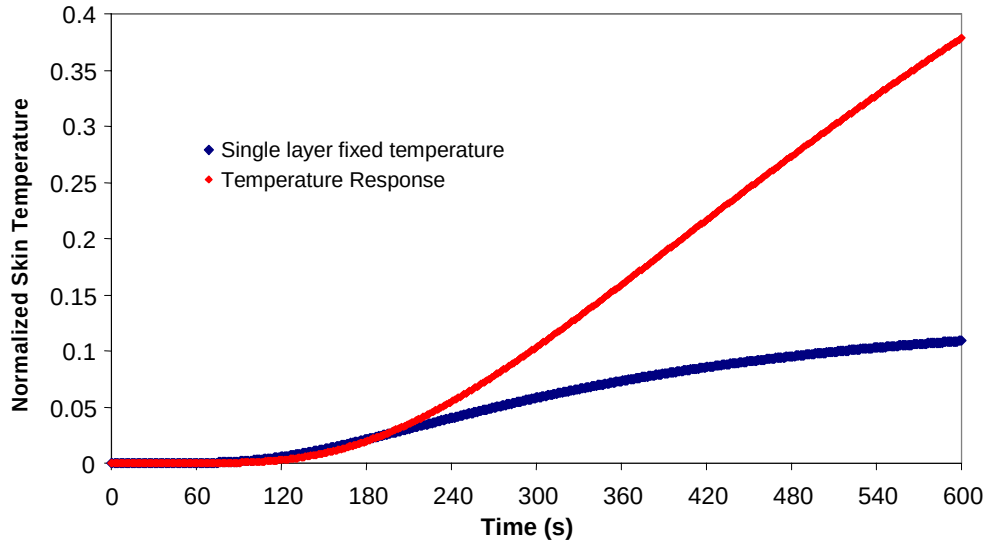

Figure 4.5 – Single layer assumption with fixed temperatures with gear thickness of 20 mm and skin thickness of 3 mm

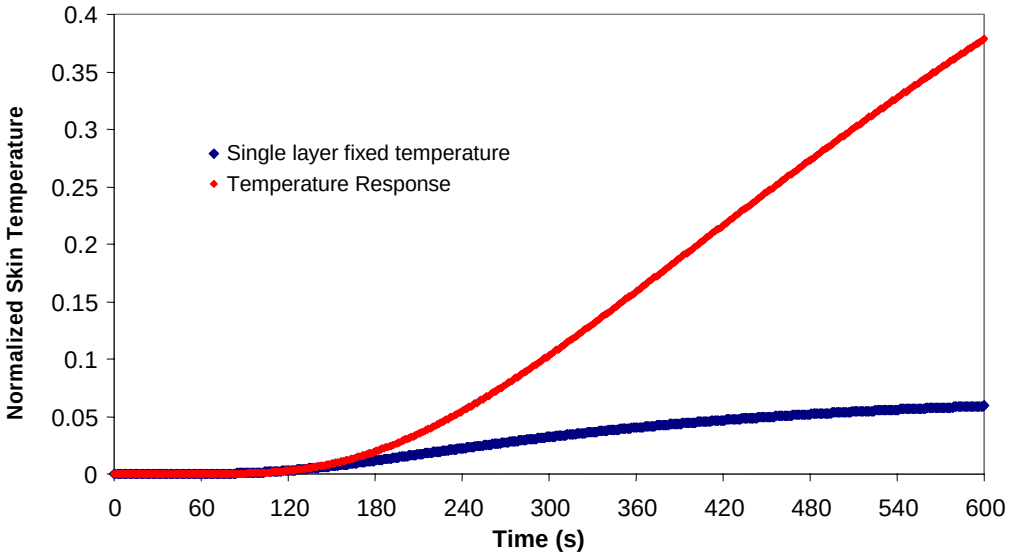

Figure 4.6 – Single layer assumption with fixed temperatures with gear thickness of 40 mm and skin thickness of 3 mm

The resulting graphs show that the calculation asymptotes to a temperature of 0.12 for a thickness of 20 mm and to 0.07 for a thickness of 40 mm. This is because of the boundary conditions of the program. The final solution of the program, when $t = \infty$, is a

straight line between point (0, 0) and point (l , 1). From the slope of this line, the maximum temperature value for a given point can be determined, which in this instance is a maximum of 0.07 for a point of 3 mm in a 43 mm system. Another limitation is that the calculation does not take into account that the thermal diffusivity of the skin is smaller than that seen in the gear. In order to compensate for these calculation limitations, the skin thickness is increased to an equivalent skin thickness and a single thermal diffusivity value can be used for both the skin and the gear. This equivalent skin thickness is found from a ratio of thermal diffusivities and thicknesses, and solved as seen in Equation 4.1.

$$L_{s_{equiv}} = \sqrt{\frac{\alpha_G}{\alpha_S}} \cdot L_s \tag{4.1}$$

where;

$L_{s_{equiv}} = equivalent\ skin\ thickness\,[mm]$

$L_s = actual\ skin\ thickness\ [mm]$

$\alpha_G = gear\ thermal\ diffusivity\ [m^2/s]$

$\alpha_S = skin\ thermal\ diffusivity\ [m^2/s]$

$$L_{s_{equiv}} = \sqrt{\frac{2.2E-7\,\mathrm{m}^2/s}{5E-8\,m^2/s}} \cdot 3mm \approx 7mm \tag{4.2}$$

From the calculation the skin thickness is increased from 3mm to 7 mm in the 20 mm system and from 3 mm to 17 mm in the 40 mm system. The equivalent length for the skin compensates for the calculation's limitation and allows for the use of a single

thermal diffusivity value. The solution is recalculated with these thicknesses and the results are seen in Figure 4.7.

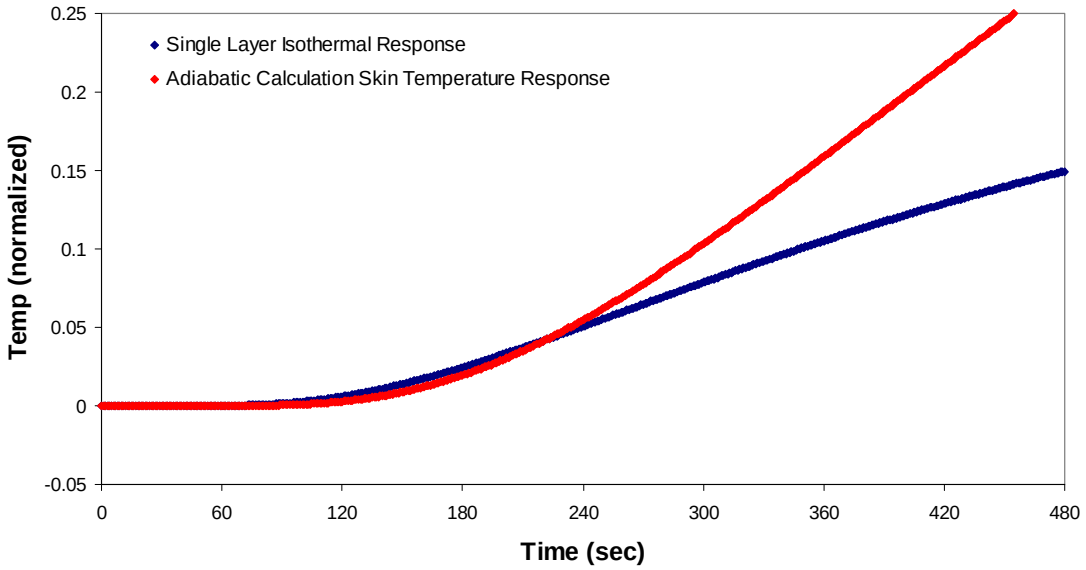

Figure 4.7 – Skin temperature response using single layer assumption with fixed temperatures for gear thickness of 20 mm and 40 mm compared to best fit adiabatic temperature calculation

The best representative response from this calculation is found with a thermal diffusivity value of 2.2E-7 m^2/s and 8.8E-7 m^2/s for gear thicknesses of 20 mm and 40 mm respectively. The responses of the two thicknesses are identical and have a time delay of 138 seconds and reach a temperature of 0.1 at 337 seconds, which are both within the described range. These results for both thicknesses correspond to an α / l^2 value of 5.5E-4 s^{-1} for the gear. When compared to the best fit curve as described before, the slopes of the skin temperature response differ where the best fit curve response's slope is higher than that of the single layer with fixed temperature response. This difference is due to the boundary condition assumptions in that the best fit curve calculation is an adiabatic

consideration, where there is a zero flux condition at the skin, and the single layer assumption is an isothermal consideration, where there is a fixed core body temperature. The two responses are compared to the test data in Figure 4.8.

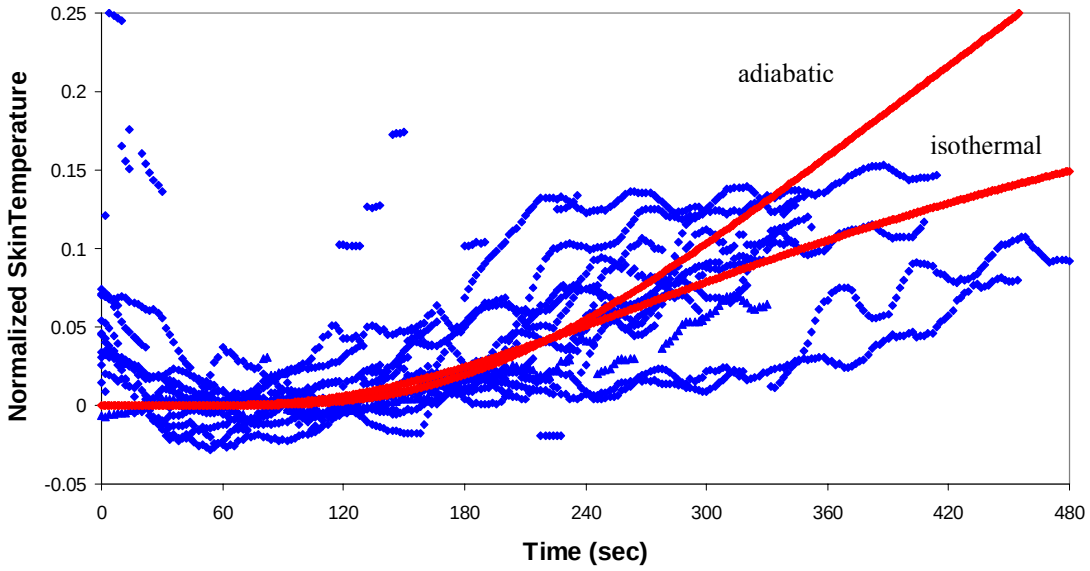

Figure 4.8 – Temperature response for single layer assumption compared to test data

The two calculations are both representative of the skin temperature response when considering the early portions of the temperature rise and the target time ranges previously described. However, the isothermal single layer assumption response has a milder transient in the long term and overall describes the temperature delay and rise phenomenon for the heating condition of the testing data better than the adiabatic consideration. This difference between the isothermal and adiabatic responses is further investigated with additional programs.

Single Layer Assumption with Ramping Temperature

The second single layer assumption uses the tri-diagonal function to solve for the energy transport and temperature at the skin surface. This calculation is also an isothermal consideration but unlike the previous single layer assumption, the temperature rise of the outermost point follows a ramping function as defined earlier and observed from the tests. The 'single layer assumption' term refers to the gear layers not including the skin. For this particular program, the skin's thickness and its alpha value are defined separately than that of the gear. The point of interest, being the skin's surface, is then located between these two defined layers. As with the previous program, the data results are attempted to be duplicated at gear thicknesses of 20 mm and 40 mm. The values for the time at the temperature locations of 0.01 and 0.1 are found from the graph using the zoom function to create a detailed grid size for determining accurate time values at these points.

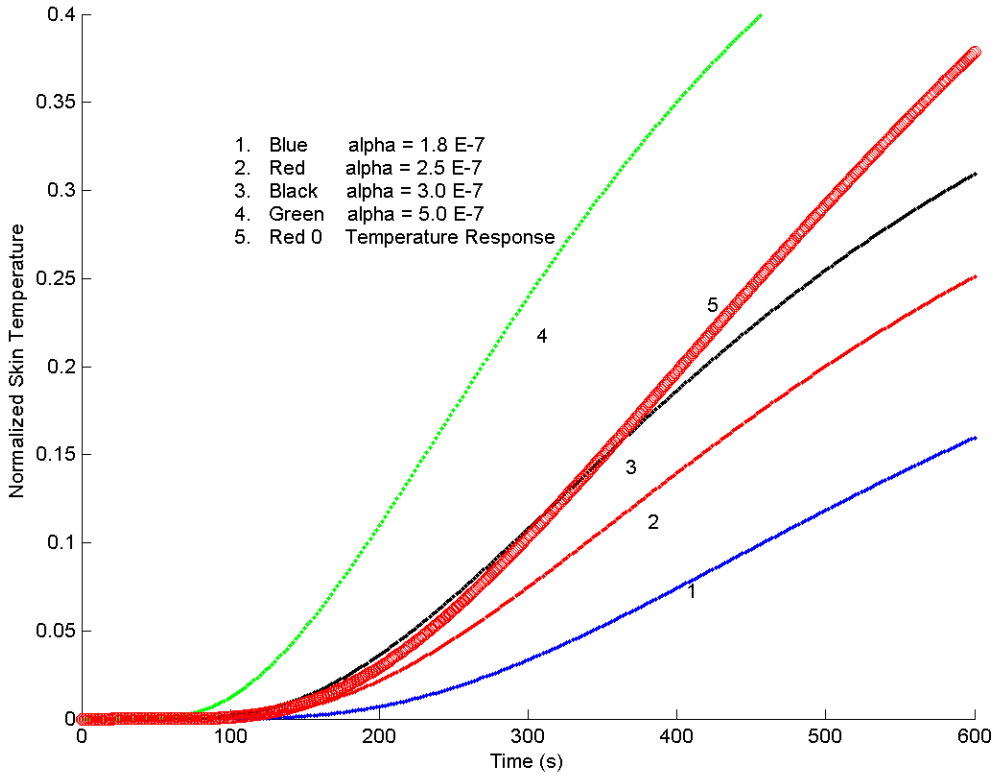

Figure 4.9 – Skin temperature response using single layer assumption with ramping temperature for gear of thickness of 20 mm

Table 4.1 – Results summary of single layer assumption with ramping temperature for 20 mm gear thickness

Number	Color	Thermal diffusivity (α)	α / l^2	Time delay (s)	Time to reach temperature 0.1 (s)
1	Blue	1.8 E-7	4.5 E-4	215	460
2	Red	2.5 E-7	6.3 E-4	165	340
3	Black	3.0 E-7	7.5 E-4	140	290
4	Green	5.0 E-7	1.3 E-3	95	190

For this single layer assumption with a gear thickness of 20 mm, a thermal diffusivity between 3.0 E-7 m^2/s and 5.0 E-7 m^2/s best describes the time delay range as seen in the testing data. However, it is seen that for the thermal diffusivity of 5.0 E-7 m^2/s the time

for which the skin temperature reaches 0.1 is 190 seconds, which is 110 seconds earlier than seen in the data. The thermal diffusivity range from 2.5 E-7 m^2/s to 3.0 E-7 m^2/s best defines the testing data for the time to reach a temperature of 0.1. However, it is seen that the time delay associated with 2.5 E-7 m^2/s is longer than those seen at in the testing data. Therefore, it is determined that the thermal diffusivity that best describes the overall skin temperature response is 3.0 E-7 m^2/s, which corresponds to an α / l^2 value of 7.5E-4 s^{-1}. The curve's response is confirmed in the graph by its close response seen by the previously discussed best fit temperature response curve.

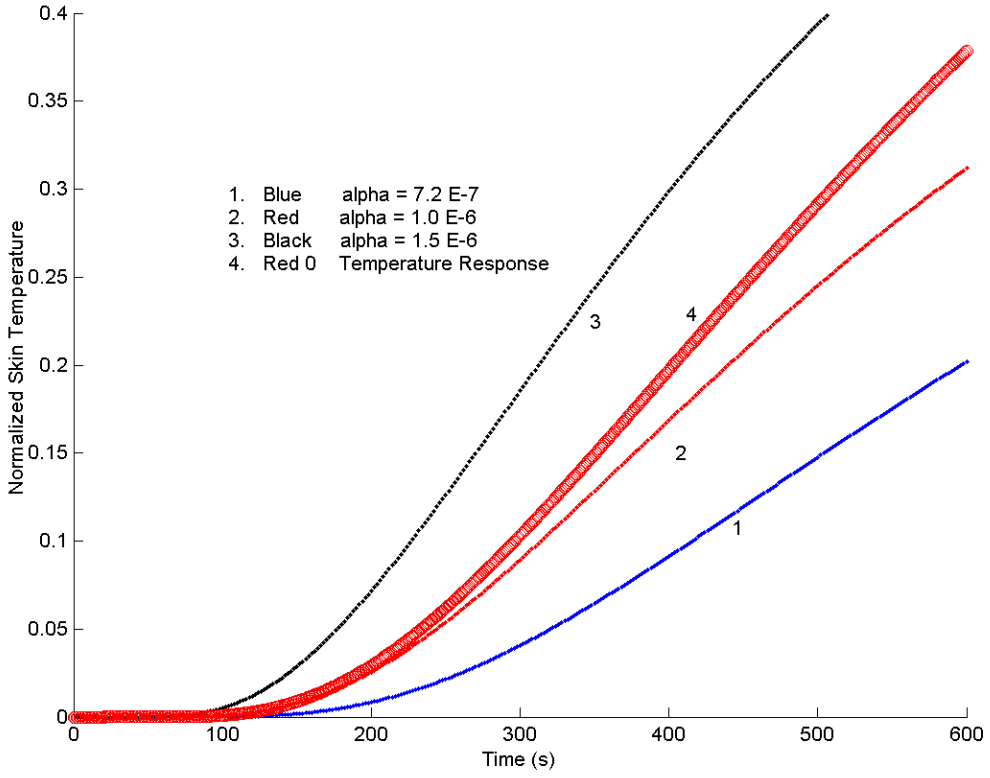

Figure 4.10 – Skin temperature response using single layer assumption with ramping temperature for gear of thickness of 40 mm

Table 4.2 – Results summary of single layer assumption with ramping temperature for 40 mm gear thickness

Number	Color	Thermal diffusivity (α)	α / l^2	Time delay (s)	Time to reach temperature 0.1 (s)
1	Blue	7.2 E-7	4.5 E-4	210	415
2	Red	1.0 E-6	6.3 E-4	160	315
3	Black	1.5 E-6	9.4 E-4	150	225

For a 40 mm system, a thermal diffusivity value of 1.0 E-6 m^2/s best describes the time to reach a temperature of 0.1 and a thermal diffusivity of 1.5 E-6 m^2/s matches the time delay more closely. When the graphs are compared to the actual response best fit curve, it is seen that the thermal diffusivity of 1.0 E-6 m^2/s is the best representative curve. This thermal diffusivity corresponds to an α / l^2 value of 6.3 E-4 s^{-1}, which is seen to be slightly higher than that found from the best fit curve of 5.5 E-4 s^{-1}. These results support the results found with the 20 mm gear thickness in that the α / l^2 value is slightly higher than that calculated from the original value.

The calculated temperature response for the 40 mm gear thickness with a thermal diffusivity of 1.0 E-6 m^2/s is compared to a set of test data temperatures. The gear thickness of 40 mm is used because the thermocouples on the subjects during the tests were in an uncompressed location on the gear. Both the outside gear temperature response and the skin temperature response are compared in Figure 4.11.

The model is run according to the times seen in the test data set. This includes a heat exposure time of 270 seconds and a cool down of an additional 80 seconds. For this particular set of data, the outside gear temperature data has an average of a 40 second

delay as compared to the calculated outside gear temperature. This delay corresponds to an average temperature difference of 0.2 or 16°C at a given time. The calculated skin temperature response accurately predicts the results seen in the tests and the results fluctuate within a normalized temperature of 0.035 or 3°C.

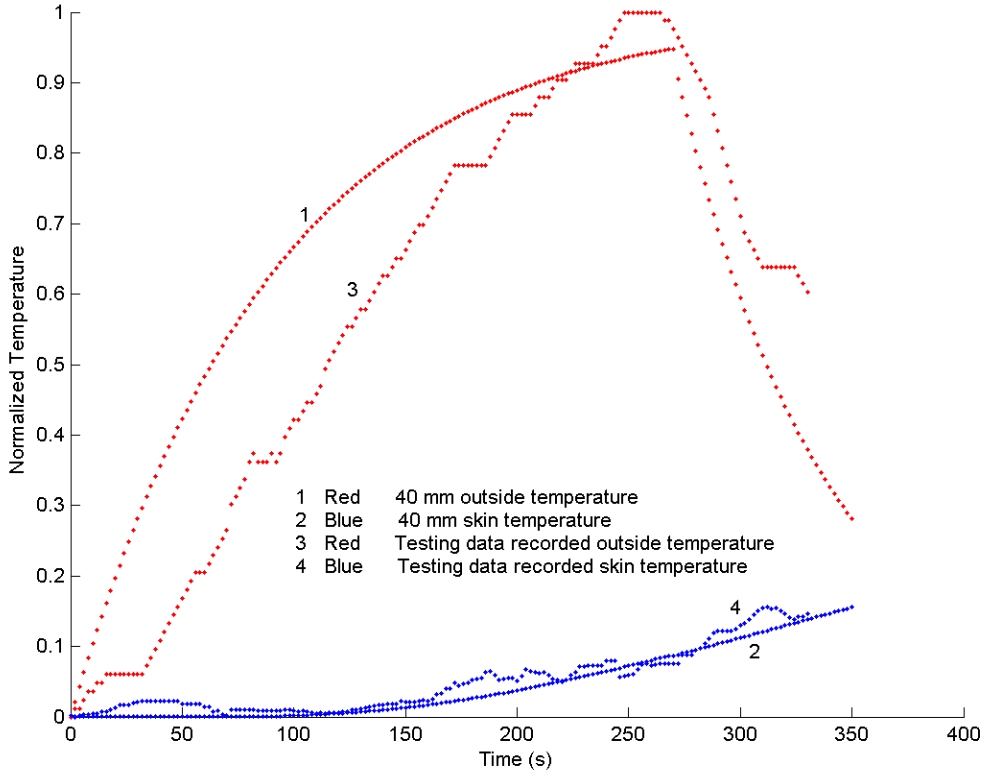

Figure 4.11 – Comparison of calculated isothermal response to recorded testing data

Overall, the single layer assumption with a ramping outside temperature is able to produce results that match the critical ranges associate with the testing results. Because of the defined boundary conditions and the use of two layers, one for the skin and one for

the gear, the temperature results were not constrained to an asymptotic value as seen in the single layer assumption with fixed temperatures.

The two calculations show that the slope of the skin temperature response is slightly less in the models than that seen in the best fit curve. However, the results of both programs match the previously discussed critical ranges seen in the data. The variations between the two models are related to the differences in the boundary conditions for the adiabatic and isothermal assumptions. In the MATLAB single layer assumption, the core body temperature is considered constant at 37°C, where in the case of the best fit curve the inner temperature is not fixed. The MATLAB program also assumes that the skin responds to the temperature according to its properties, rather than assuming the same thermal diffusivity of the gear

To more completely describe the difference between the adiabatic and isothermal calculations, a long term calculation with both heating and cooling are compared. The input values for the adiabatic calculation are described earlier for the best fit curve and the inputs for the isothermal calculation include a thickness of 40 mm and a thermal diffusivity of 1 E-6 m^2/s. First, a heat exposure of 5 minutes (300 seconds) with cooling for an additional 10 minutes (600 seconds) is considered. This heat exposure time is based on the average time that the firefighters remained in the heat exposure during the live fire tests. In the second comparison, the heat exposure is considered for 10 minutes (600 seconds) with cool down of 5 minutes (300 seconds). This long heat exposure is to

observe the differences in the calculations for an extended time frame. These comparisons are displayed in Figures 4.12 and 4.13.

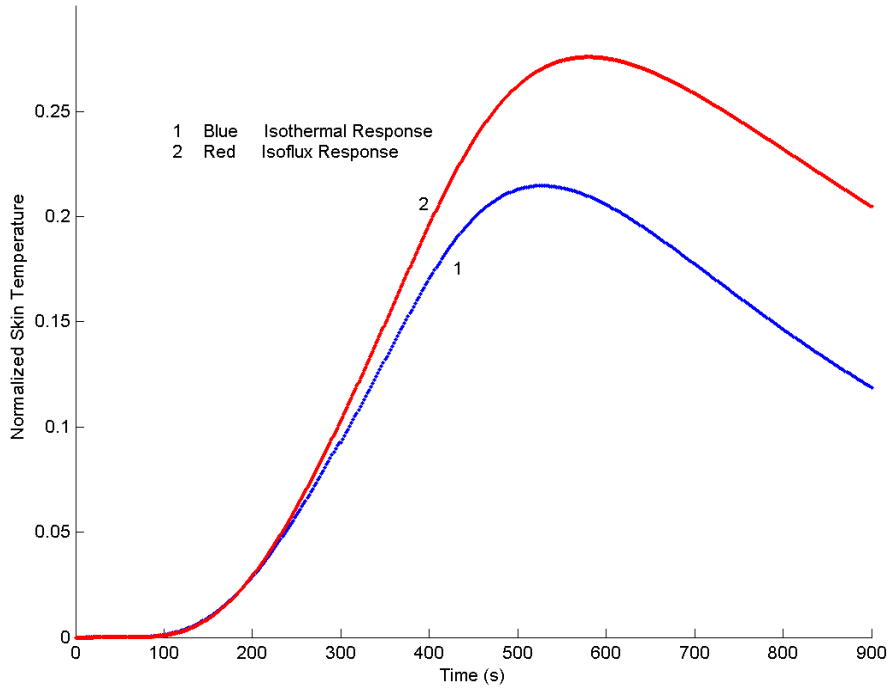

Figure 4.12 – Comparison of isothermal and adiabatic calculations for a 300 second heat exposure and a 600 second cool down

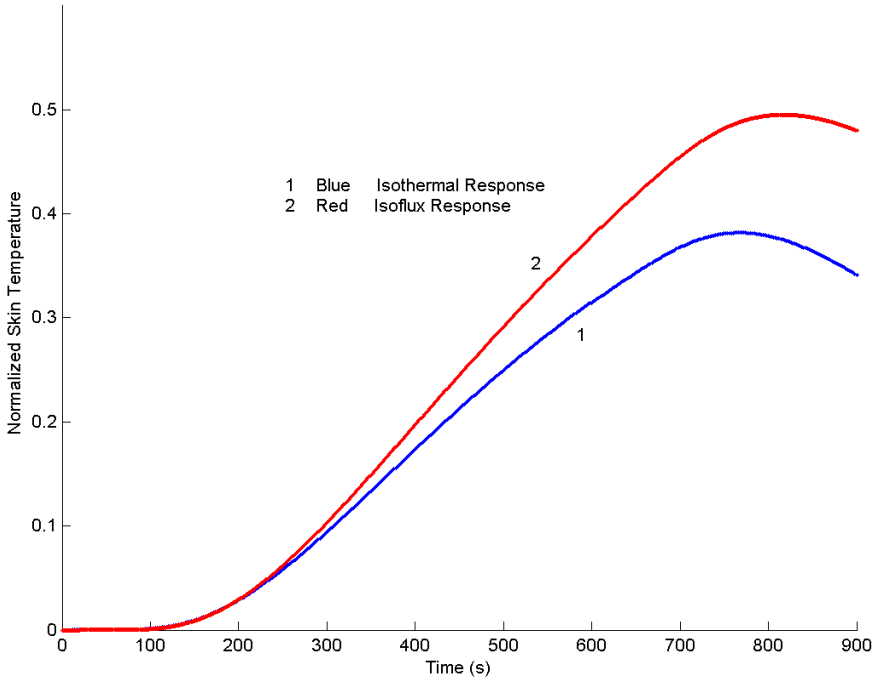

Figure 4.13 – Comparison of isothermal and adiabatic calculations for a 600 second heat exposure and a 300 second cool down

As discussed earlier, the two calculations reproduce similar responses for the initial temperature rise. However, the isothermal calculation produces a response with a milder transient in the long term, and this smaller slope gives an overall better representation of the testing data. Comments from the test subjects noted that the HUD warning lights had a faster response than desired to the heat, which is explained by the larger slope and higher peak temperature of the adiabatic calculation. Therefore, it is suggested that the algorithm used in the data collecting device to predict the time until burned should be changed from an adiabatic assumption to an isothermal assumption. The calculated response will be slightly slower and give a better predicted time until the subject is burned.

Multi-Layered Model

The multi-layered system model also uses a tri-diagonal solver to complete the calculation. Layer inputs are defined and material properties are used to calculate the thermal diffusivity of each of the layers. The first calculation uses only six layers with no air gaps to understand the straight material contribution to the energy transport. These layers include; skin, heavy t-shirt, sweatshirt, thermal barrier, moisture barrier and outer shell.

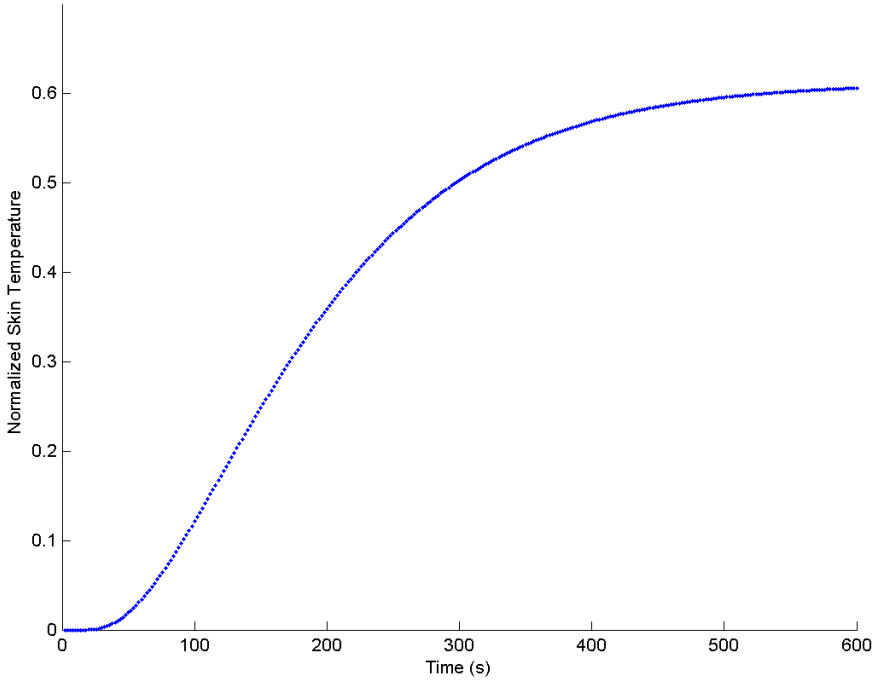

Figure 4.14 – Skin temperature response from multi-layered system without air gaps

Table 4.3 – Results summary of 6 layered multi-layer model

Number of layers	layers	Time delay (s)	Time to reach temperature 0.1 (s)
6	Skin, heavy t-shirt, sweatshirt, thermal barrier, moisture barrier, outer shell	42	90

The system has a short time delay of 42 seconds with a very rapid response and a high peak temperature. The single layer assumption with ramping temperatures is used to find a curve fit for these results. This correlation determines how closely the two programs are related and if the multi-layered solution can be summarized with a single thermal diffusivity value in a single layer assumption. The results are compared in Figure 4.15.

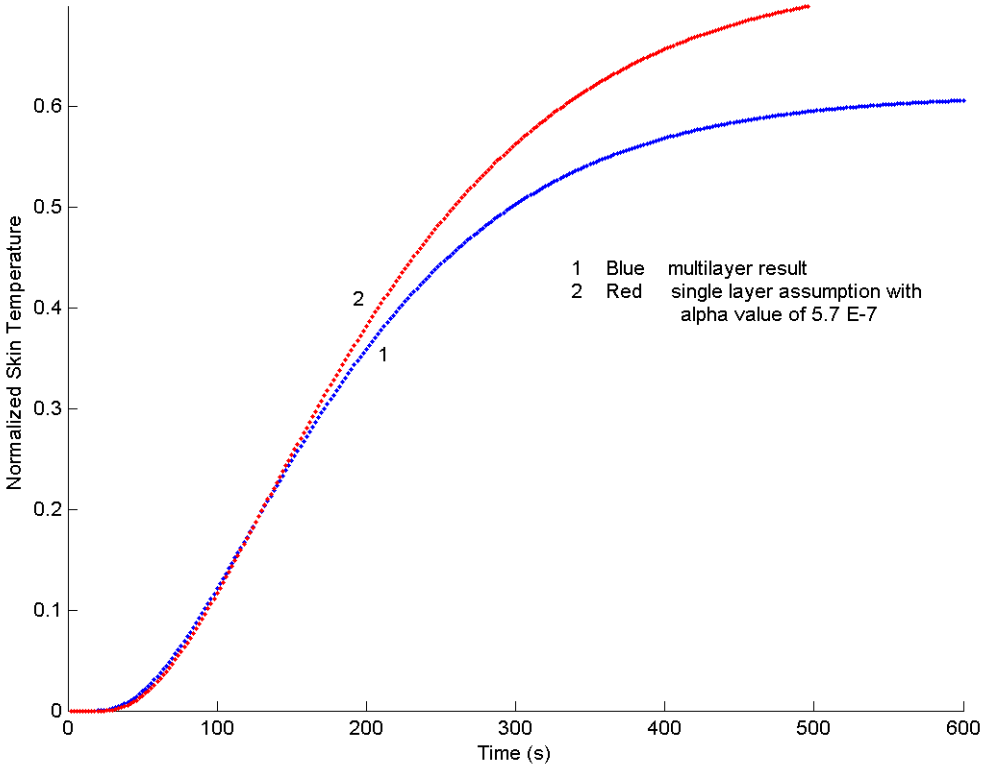

Figure 4.15 – Correlation of single layer assumption and multi-layer model results

The thickness of the original multi-layer model is found to be 15.4 mm, giving a gear thickness of 12.4 mm. Using this thickness for the single layer assumption, a thermal diffusivity of 5.7 E-7 m^2/s best represents the results found by the multi-layer model. The results have a difference of 2 seconds at both temperatures of 0.01 and 0.1. The

results deviate from each other at higher temperatures, starting at an estimated temperature of 0.4. However, these high temperatures are not relevant to this study because skin temperatures do not reach this level and the deviation between the graphs becomes much smaller when more realistic skin temperatures are reproduced. Therefore, it is found that the multi-layered system can be represented as a single layer assumption with a ramping temperature function because of their close comparison at temperatures less than 0.4.

An area of interest for the inaccuracy of the multi-layer calculation is in the thickness values used for the layers. Most of the thicknesses are of assumed accuracy from measurements recorded in NIST reports. At a fiber level, the actual location of the start of material can vary, especially with material movement and the aging of the material. The effect of the accuracy of the material thicknesses is further investigated.

The same layer configuration is used, except that the thicknesses of the materials are increased by percentages to observe how the skin surface temperature response changes. It is seen in Figure 4.16 that the material thicknesses need to be increased by 75% to obtain the results seen in the tests. This margin of error for the material properties is unrealistic and therefore indicates that the presence of air gaps is critical in the protection value of the protective gear.

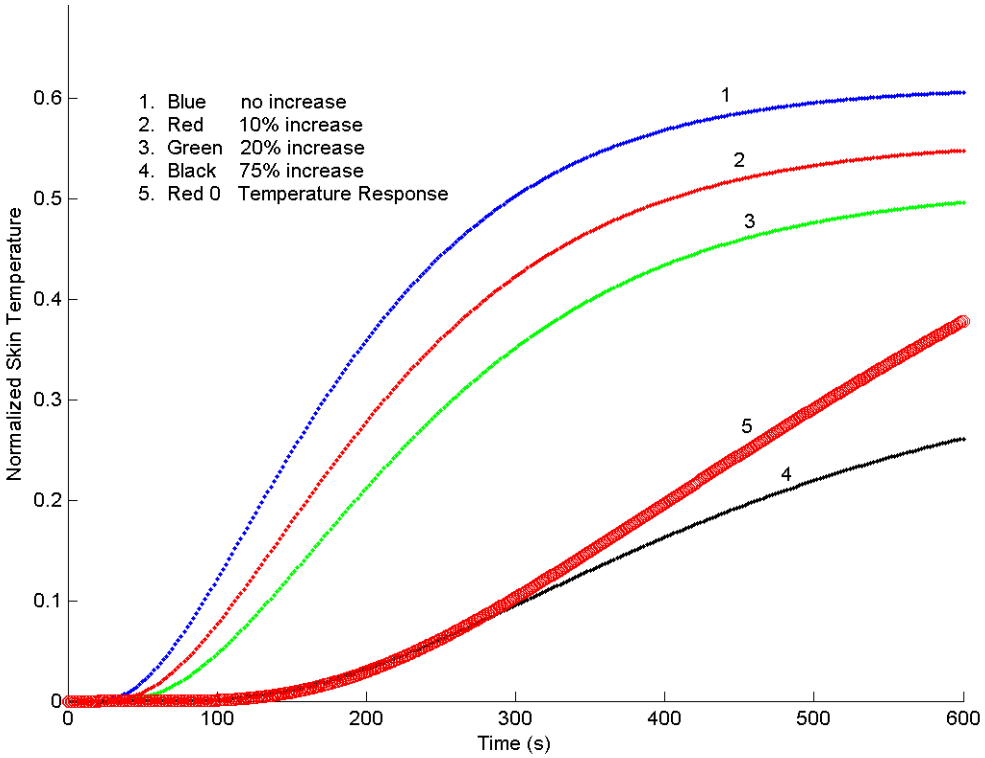

Figure 4.16 – Skin temperature response with increasing material thickness from multi-layered system without air gaps

Table 4.4 – Percentage increase results for 6 layer system comprised of; Skin, heavy t-shirt, sweatshirt, thermal barrier, moisture barrier, outer shell

Number of layers	Percentage increase	Time delay (s)	Time to reach temperature 0.1 (s)
6	0%	42	90
6	10%	52	110
6	20%	64	135
6	75%	145	308

From the estimated thickness of the diameter calculations, air gaps are able to be added to the previous system. Their location throughout the system is determined by expert judgment from the inspection of the gear and how it conforms to the body. The gear layer configuration for a 20 mm system is as follows; skin, t-shirt, 2 mm air gap,

sweatshirt, 4 mm air gap, thermal barrier, 2 mm air gap, moisture barrier, 2 mm air gap, and outer shell. For the 40 mm system, the air gap positions stay the same, but their thicknesses increase to 4 mm, 15 mm, 10 mm and 4 mm from the innermost layer out. The resulting skin temperature responses are in Figure 4.17.

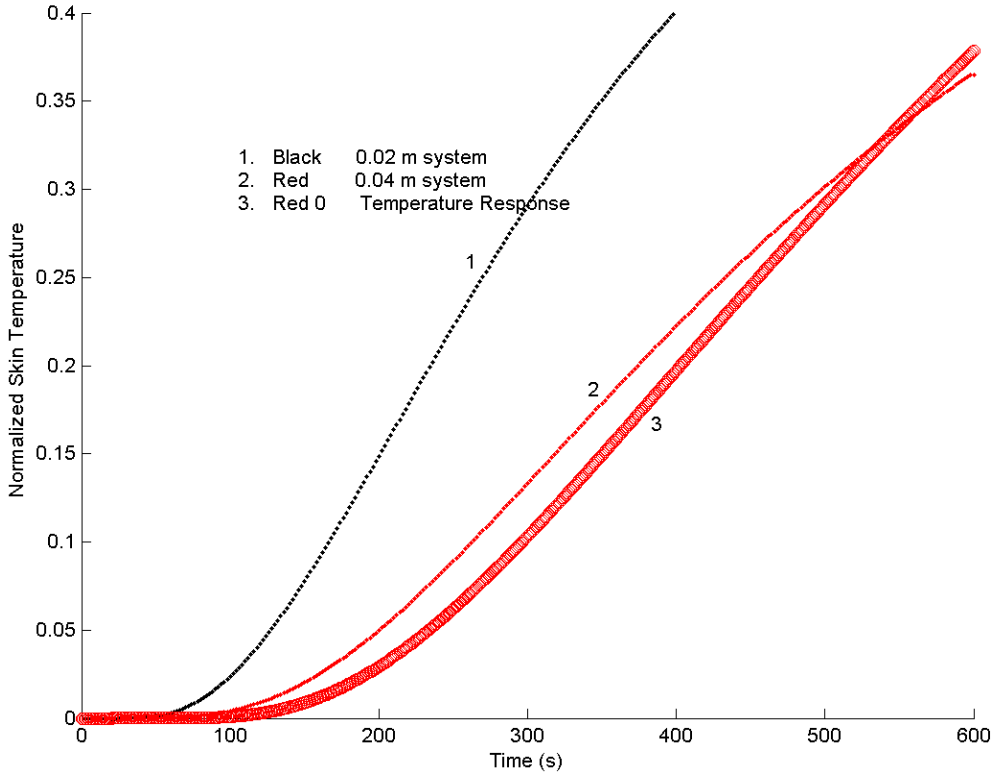

Figure 4.17 – Skin temperature response from multi-layered system with air gaps and total gear thicknesses of 20 mm and 40 mm

Table 4.5 – Results summary of multi-layer calculation including air gaps for a 20 mm and 40 mm system

Total thickness (m)	layers	Time delay (s)	Time to reach temperature 0.1 (s)
0.02	skin, t-shirt, 2 mm air gap, sweatshirt, 6 mm air gap, thermal barrier, 3 mm air gap, moisture barrier, 2 mm air gap, outer shell	79	166
0.04	skin, t-shirt, 4 mm air gap, sweatshirt, 15 mm air gap, thermal barrier, 10 mm air gap, moisture barrier, 4 mm air gap, outer shell	124	262

The addition of the air gaps has a significant impact on the system's performance. For the 20 mm system, the time delay increases by 37 seconds and the time to a temperature of 0.1 increases by 76 seconds. For the 40 mm system, the time delay increases by 82 seconds and the time to temperature 0.1 increases by 172 seconds. These results show that a system of layers must consider the presence of the air gaps to understand its performance. The result for the 40 mm system is close to duplicating the testing results however, the time delay is still short and doesn't quite match the results of the best fit curve.

To replicate the results obtained in the testing, the air gaps and a reasonable material thickness increase are both taken into account. A reasonable margin of error for the material thicknesses is considered to be 10%, which is a difference of ~0.4 mm for the thickest material (thermal barrier) and ~0.08 mm for the thin materials (moisture barrier and outer shell). The result of the combined air gaps and thickness increase is displayed in Figure 4.18, and can be compared to the air gap response and best fit curve.

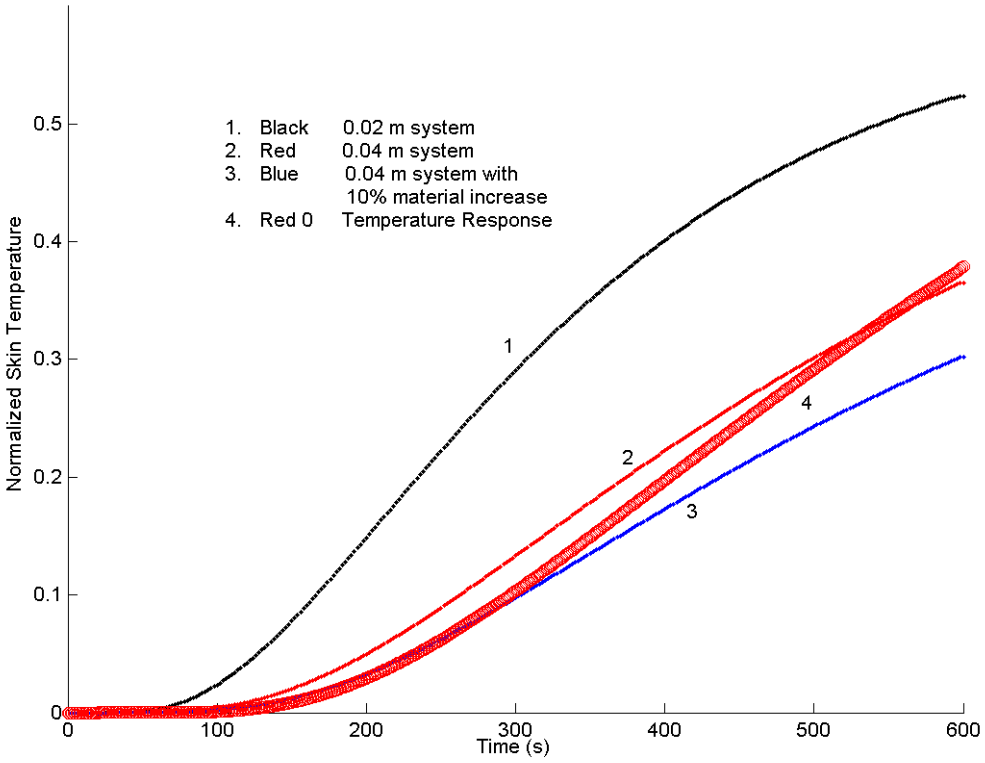

Figure 4.18 – Skin temperature response from multi-layer system with air gaps and a material increase of 10%

Table 4.6 – Results summary for multi-layer system with air gaps and thickness increase

Number	Color	Thickness (m)	Percent increase	Time delay (s)	Time to reach temperature 0.1 (s)
1	Black	0.02	0%	79	166
2	Red	0.04	0%	124	262
3	Blue	0.04	10%	142	303

The result from combining both the air gaps and a material increase is an accurate representation of the skin temperature response in the testing data. The time delay is found within the range at 142 seconds and a time to temperature 0.1 at 303 seconds. The response deviates from the best fit curve at later times like the other isothermal calculations because of the difference in assumptions between the programs.

The single layer assumption is used to determine a matching thermal diffusivity value for describing this system. For the multi-layer calculation, the total air gap thickness was kept constant at 33 mm while only the material thicknesses were increased by 10%. Because it is such a small percentage increase, the total gear thickness only increases by 0.7 mm for a total gear thickness of 41 mm, which is used in the single layer assumption comparison.

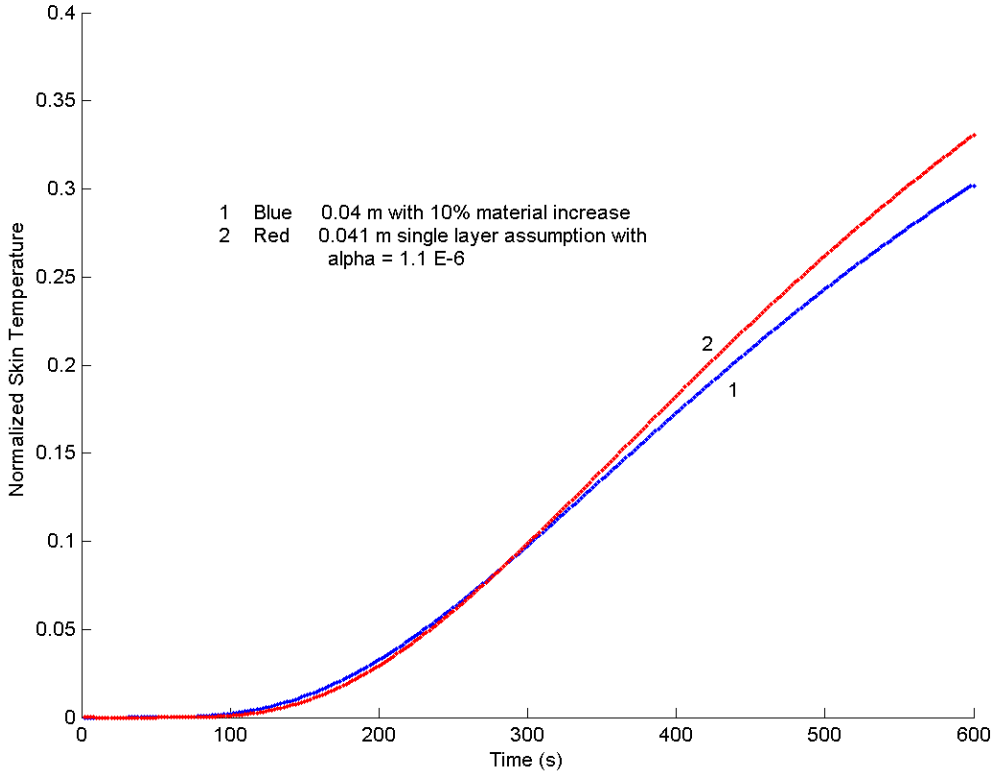

Figure 4.19 – Determining thermal diffusivity value of multi-layer system by matching results with single layer assumption

Table 4.7 – Results summary for single layer assumption match to multi-layer result

Number	Color	Program	Thermal diffusivity	Time delay (s)	Time to reach temperature 0.1 (s)
1	Blue	Multi-layer		142	303
2	Red	Single layer	1.1 E-6	152	302

It is determined from the single layer assumption that the thermal diffusivity of the multi-layered system that includes air gaps and a 10% increase in material thicknesses is 1.1 E-6 m^2/s. From the gear thickness of 41 mm, an α/l^2 value of 6.5 E-4 s^{-1} is determined for the overall multi-layered gear system that best represents the results from the testing data. As noted before, it is assumed that a thickness of 40 mm is best representative of the testing results because of the location of the thermocouples. A thickness of 20 mm is more representative of the compressed areas of the gear, such as around the straps of the SCBA. Additional testing with thermocouple data recorded at these compressed locations should be completed and compared to the model's results at the 20 mm thickness.

It is seen in the results above that the air gap has a significant influence on the multi-layered system. The original placement and thickness associated at each location was determined through educated estimations from gear inspection. However, the actual thickness of each air gap could not be directly measured, so the total air gap thickness was divided among the determined locations. Therefore, calculations are completed to determine if varying the thickness at each location has a significant impact on the system as well.

There are two specific gaps of interest which include; the gap between the sweatshirt and the thermal barrier, and the gap between the thermal barrier and the moisture barrier. These are of specific interest because they are the two gaps that are most likely to vary. The t-shirt is assumed to be located directly against the skin and the t-shirt and sweatshirt

can only separate a little because of the weight of the additional material compressing them together. The outer shell also has minimal separation from the moisture barrier because of the gear construction. The comparison model assumes a 40 mm total gear thickness, giving a total air gap thickness of 33 mm which is distributed throughout the four locations to observe the effect.

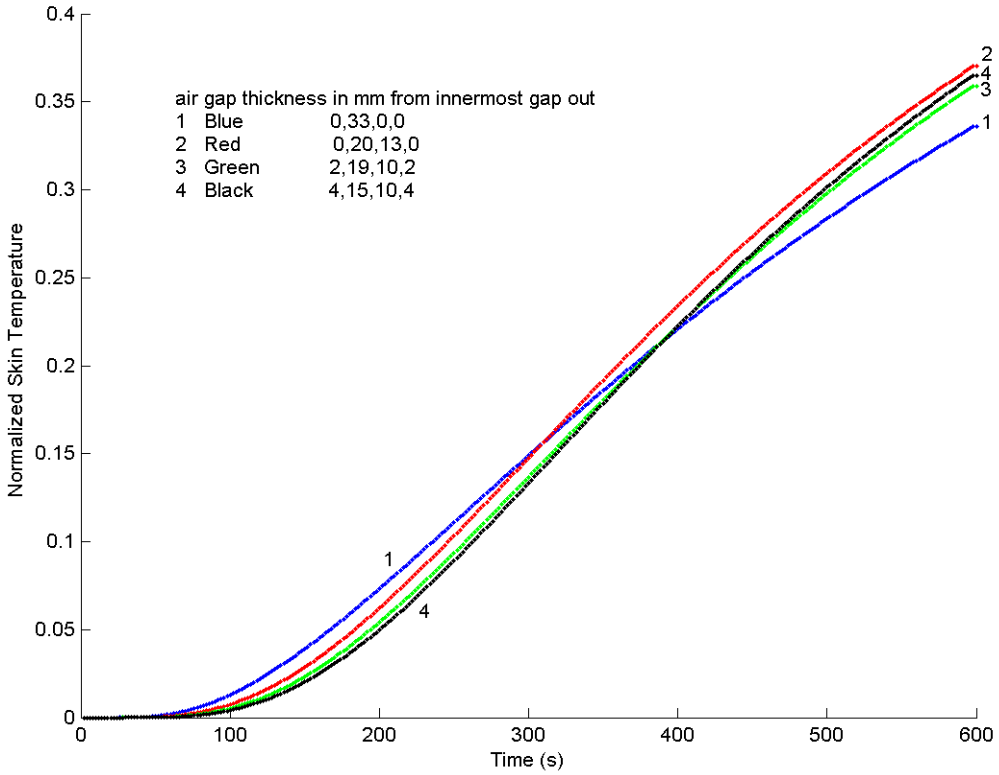

Figure 4.20 – Comparison of altering air gap thickness between four locations within a 40 mm system

Table 4.8 – Results summary for altering air gap location and location thicknesses

Number	Color	Air gap thickness at locations (mm)	Time delay (s)	Time to reach temperature 0.1 (s)
1	Blue	0,33,0,0	92	236
2	Red	0,20,13,0	108	246
3	Green	2,19,10,2	118	258
4	Black	4,15,10,4	124	263

It is seen from the graph that the same total thickness of air gap distributed differently throughout the system creates slightly varying results. By comparing the time to reach temperatures of 0.01 and 0.1, a quantifiable difference can be made and shows how the air gap alterations affect both the time delay and the slope of the temperature response. The most significant result is that the time delay increases as the number of air gaps increase and is largest when the total air gap thickness is more evenly distributed between the four locations. The slopes of the graphs are consistent according to each other for the first 350 seconds to a temperature of about 0.2. After this, the single air gap system has the smallest slope and the system with the most distributed air gaps has the highest slope. It is determined from the time delay and from the response in the first 300 seconds that it is more effective to have multiple air gaps of smaller thickness than a single large air gap.

The contribution of the air gap on the system is mathematically investigated through its properties and heat transfer equations to understand how it relates to the energy transport. Additional graphs from the multi-layer model can assist in deducing the actual role of an air gap and what aspects of the energy transport it influences.

The thermal diffusivity of an air gap can be determined from air's density, thermal conductivity and specific heat. For air properties at a temperature of 50 °C, a calculated thermal diffusivity is found to be 2.4×10^{-5} m^2/s. This value is 20 to 200 times greater than the thermal diffusivity values calculated for the other firefighting materials, which is due to the very low density of the air gap. The high thermal diffusivity can be easily observed by the side profile graph of the temperature distribution though the different

layers. The temperature is consistent across the air gap's length as represented by a straight line between nodes 123 and 283 in Figure 4.21.

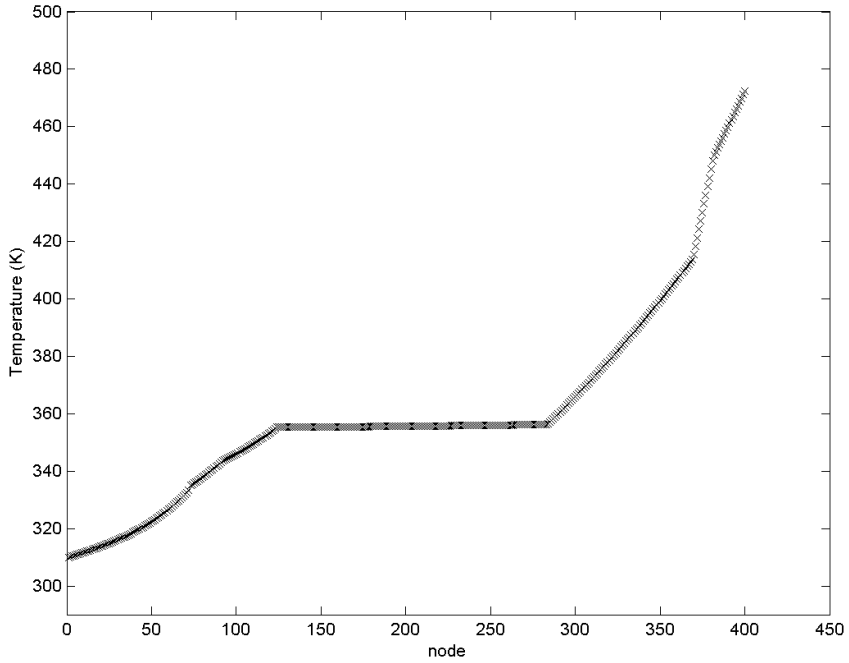

Figure 4.21 – Side profile of temperature distribution through layers. Skin is from nodes 0-50, air from nodes 123-283, outside of gear at node 400

Because of the air gap's high thermal diffusivity, it provides little to no assistance to the system in terms of resisting heat. However, the air gap adds to the system a thickness value. This becomes important when looking at the system's α/l^2 parameter associated with the characteristic time scale. Since the air gap in a system does not affect the thermal diffusivity, α, value but does increase the length, l^2, value, there will be an overall decrease in the α/l^2 parameter when an air gap is present and therefore a lower time scale constant and improved gear performance.

The multi-layered system program cannot currently be used to predict the actual skin temperature and behavior of a multi-layered system through direct input of different layers, but provides insight to the different layer contributions. This is because of assumptions used for mathematical purposes and external variables in actual applications. One assumption that affects its accuracy is that the calculation assumes a laminar, two dimensional model, where in full scale practicality, the system is three dimensional and in motion. The constant movement causes variations in the clothing and air gap thicknesses which enhance lateral air movement and temperature distribution around and out of the system.

Another major variation in the system is the evaporation and vapor transportation from water in the system. During practical exercises, a person will perspire and add water to the overall system. This water in the system can alter property values for the materials and also absorb heat through the evaporation process. The water vapor enhances energy transport laterally within and out of the system as previously discussed with the air movement. Even though the multi-layered program cannot be used to predict actual clothing response, it provides useful insight to the contribution of each individual layer, specifically that of the air gaps.

Chapter V: Conclusions

Conclusions

This study provided a better understanding of the temperature response and energy transport in firefighter gear during high heat exposures through full scale testing and mathematical modeling. The testing results provided a background for the mathematical calculations of the energy transport through the gear which lead to an understanding of the contribution of the various layers of the gear.

It was determined that a single layer assumption with two fixed temperatures can be used to determine the skin temperature response of the data. The calculation is limited when the point of interest is much smaller than the overall thickness and the skin's thermal diffusivity is not taken into account. Therefore, an equivalent skin thickness must be found in order to use a single thermal diffusivity value for the calculation. For the gear thicknesses of 20 mm and 40 mm, skin thickness equivalents of 7 mm and 17 mm are found to account for the limitation. Thermal diffusivity values of 2.2 E-7 m^2/s and 8.8 E-7 m^2/s for gear thicknesses of 20 mm and 40 mm, respectively, were determined as best representative responses of the testing data. These results both correspond to an α/l^2 value of 5.5E-4 s^{-1} for the overall gear, which is also what was determined by a best fit curve calculation. The slight variations in the two calculations are from the different assumptions and boundary conditions made for each model.

A single layer assumption with a ramping temperature associated with the outside gear response and a fixed internal temperature proved to be the best thermal model in

calculating the skin temperature response seen in the full scale tests. There are slight variations related to the slope of the temperature response, but these are associated with necessary mathematical assumptions and additional energy transport methods present in actual three dimensional firefighting clothing systems. Thermal diffusivity values of 3.0 E-7 m^2/s for a 20 mm gear thickness and 1.0 E-6 m^2/s for a 40 mm gear thickness were determined to best describe the overall skin temperature response of the testing data. When compared to a single set of testing data, the calculation for a 40 mm gear thickness predicted the skin temperature within 3.5% or 3 °C of the actual recorded skin temperature.

The isothermal assumption made by the single layer assumptions proved to create a more accurate response curve to the testing data than the adiabatic assumption initially considered. The isothermal assumption has a milder slope which leads to a slower response and a lower peak of the skin temperature in the long term calculations. It is suggested that the algorithm used to predict the skin temperature in the data collecting device be changed to an isothermal assumption in order to have more accurate results in alerting firefighters of their potential to burn.

A multi-layer model that uses material properties to determine the skin temperature response for a system provided results showing the individual contribution of layers in a multi-layered system, specifically the role of air gaps throughout firefighting gear. The model cannot currently predict an accurate skin temperature response by raw layer input, but can reproduce testing results through reasonable input manipulation. The results

from the model can be compared to the single layer assumption model with a ramping temperature, proving that the multi-layered firefighting gear can be represented by the single layer assumption. Results from the multi-layered system determined a thermal diffusivity value of 1.1 E-6 m^2/s for a 41 mm gear thickness, which corresponds to an α/l^2 value of 6.5E-4 s^{-1} for the gear.

The study shows conclusive evidence that air gaps positioned between layers of firefighting gear provide a significant amount of protection to the firefighter. The air gap specifically contributes to the thickness of the gear and not its thermal diffusivity. This is significant in lowering the α/l^2 parameter, which is associated with the characteristic time scale in calculations, resulting in a longer delay in the heat wave reaching the skin's surface.

The results from rearranging the position of the air gaps throughout the system were not definitive. However, slight variations suggest that it may be more effective to have multiple air gaps of smaller thickness throughout the gear than a single air gap of large thickness. In actual fire scenarios, these air gaps also provide avenues for the three dimensional dispersing of energy around and out of the system, enhancing the thermal protection to the firefighter.

Future Work

In order to continue to improve firefighter and personnel safety, research must continue to strive to further understand firefighting scenarios. Subject matters of interest within the field include; quantifying actual thermal firefighting conditions, understanding the process within the personal protective layers and identifying additional mechanisms contributing to heat transfer. The deeper the understanding of the subject as a whole, the more productive we can be with firefighter education and safety system development.

To date, there is no data that reflects the actual conditions that firefighters face while in the line of duty. All conditions for these studies and previous studies have been manifested through regulated test scenarios. It is important to understand the level of heat exposure and duration times that firefighters face during actual fires.

Currently, a study is being developed and implemented that will collect temperature data for live fire events. The study is being conducted in conjunction with fire departments throughout the Washington, D.C metropolitan area. Multiple fire departments with high fire call volumes are participating in the study, which will provide a higher likelihood for data collecting opportunities. A thermocouple and data collecting device is being developed which is non-invasive and connected to the SCBA of an apparatus' officer and/or nozzle man. These two individuals have the highest likelihood of being introduced to the intense heat during a fire and provide quality data samples.

The mathematical calculations of the temperature distribution through a multi-layered system are based on given material properties and thermal dynamic theories. Further research that uses multiple thermocouples dispersed throughout turn out gear would provide experimental data that could relate to and improve the multi-layered calculations. Supporting data and accurate material properties could lead to the ability to predict actual performance and thermal response of a given set of materials.

Some environmental factors present in actual firefighting scenarios were not taken into account for this study. One important factor is the presence of a heat sink and effects of evaporation within the gear. Because of physical demands of structural firefighting, firefighters perspire, introducing water saturated material layers to the PPE. The water will absorb some of the energy leading to evaporation, acting as a heat sink and adding additional protection from heat penetration. However, the evaporation transportation adds a negative factor to the protection to the firefighter after extended heat exposure. How these factors affect the energy transport should be further researched through theoretical modeling and experimental tests.

Appendix A: Tables and Graphs

Table A.1 – Materials and associated properties obtained from NIST reports

	Thickness	Density, ρ	specific heat, c_p	thermal conductivity, k
	m	Kg/m^3	J/Kg°C	W/m K
Cotton Duck (Outer shell)	0.0013233	518.9	1620	0.1017
Nomex III Defender (Outer shell)	0.0008204	316.9	1510	0.0679
PBI Kevlar Kombat (Outer Shell)	0.0007976	321.8	890	0.073
Breathe-Tex (Moisture Barrier)	0.00122	120.7	2280	0.0441
Breathe-Tex Plus (Moisture Barrier)	0.00111	179.4	2050	0.0461
Nomex E-89 Crosstech (Moisture Barrier)	0.0009627	143.1	1900	0.0479
Neo-Guard (Moisture Barrier)	0.0005486	597.4	1480	0.1005
Nomex III Pajama Check (Moisture Barrier)	0.0005156	316.8	1930	0.0621
Aralite (thermal liner)	0.00359	74.2	1620	0.0462
Scotchlite Trim (Trim)	0.0007493	81.6	950	0.1269
Skin	0.003	1200	3558	0.21
Cotton Shirt (Heavy)	0.00084	317	1500	0.04
Cotton Shirt (Light)	0.00056	316	1500	0.04
50/50 Cotton Polyester Sweatshirt	0.0013	269	1600	0.07
Air	0.002	1.13	1005	0.0271
Water	0.001	980	4186	0.58

Table A.2 – Caliper measured thickness of t-shirts and sweatshirt

	100% cotton thin undershirt (Hanes)		**100% Cotton pre-shrunk heavy t-shirt**		**50% Cotton 50% Polyester sweatshirt**	
1 layer	mm	in	mm	in	mm	in
slight resistance	0.559	0.022	0.8382	0.033	1.27	0.05
max resistance	0.3556	0.014	0.508	0.02	0.7112	0.028
moderate resistance	0.5334	0.021	0.7112	0.028	0.889	0.035
2 layers						
slight resistance	1.118	0.044	1.6	0.063	2.438	0.096
max resistance	0.6604	0.026	1.04	0.041	1.27	0.05
moderate resistance	0.9652	0.038	1.4	0.055	1.854	0.073
4 layers						
slight resistance	2.032	0.08	3.073	0.121	5.436	0.214
max resistance	1.3462	0.053	1.9812	0.078	2.769	0.109
moderate resistance	1.7272	0.068	2.616	0.103	3.531	0.139

Table A.3 – Calculated densities for t-shirts and sweatshirt

Densities			
100% cotton thin undershirt (Hanes)			
	volume (cm^3)	mass (g)	density (g/cm^3)
compressed	400	126.5	0.316
loose	800	126.5	0.158
100% Cotton pre-shrunk heavy t-shirt			
	volume (cm^3)	mass (g)	density (g/cm^3)
compressed	1300	412	0.317
loose	1800	412	0.229
50% Cotton 50% Polyester MFRI sweatshirt			
	volume (cm^3)	mass (g)	density (g/cm^3)
compressed	1600	430.8	0.269
loose	2500	430.8	0.172

Table A.4 – Measurements for thickness of gear when worn by a subject

Subject A								
	arm		bicep		chest		stomach	
	inches	m	inches	m	inches	m	inches	m
Circumferences								
actual/skin	8.5	0.22	10	0.25	34.5	0.88	31.5	0.80
loose gear	15.5	0.39	19.5	0.50	44	1.12	43	1.09
tight gear	10.5	0.27	13	0.33	38	0.97	35.5	0.90
Diameter								
actual/skin	2.71	0.07	3.18	0.08	10.98	0.28	10.03	0.25
loose gear	4.93	0.13	6.21	0.16	14.01	0.36	13.69	0.35
tight gear	3.34	0.08	4.14	0.11	12.10	0.31	11.30	0.29
Gear thickness								
loose gear	1.11	0.03	1.51	0.04	1.51	0.04	1.83	0.05
tight gear	0.32	0.01	0.48	0.01	0.56	0.01	0.64	0.02

Subject B								
	arm		bicep		chest		stomach	
	inches	m	inches	m	inches	m	inches	m
Circumference								
actual/skin	8.5	0.22	12	0.30	32	0.81	29	0.74
loose gear	16	0.41	20	0.51	44	1.12	39	0.99
tight gear	11	0.28	15	0.38	39	0.99	34.5	0.88
Diameter								
actual/skin	2.71	0.07	3.82	0.10	10.19	0.26	9.23	0.23
loose gear	5.09	0.13	6.37	0.16	14.01	0.36	12.41	0.32
tight gear	3.50	0.09	4.77	0.12	12.41	0.32	10.98	0.28
Gear Thickness								
loose gear	1.19	0.03	1.27	0.03	1.91	0.05	1.59	0.04
tight gear	0.40	0.01	0.48	0.01	1.11	0.03	0.88	0.02

Table A.5 – Average thicknesses at each measuring location

	arm		bicep		chest		stomach	
	inches	m	inches	m	inches	m	inches	m
Averages								
loose gear	1.15	0.03	1.39	0.04	1.71	0.04	1.71	0.04
tight gear	0.36	0.01	0.48	0.01	0.84	0.02	0.76	0.02

Table A.6 – Overall average thickness of gear from all measurement locations

Overall Average Thickness		
	inches	m
loose gear	1.49	0.04
tight gear	0.61	0.02

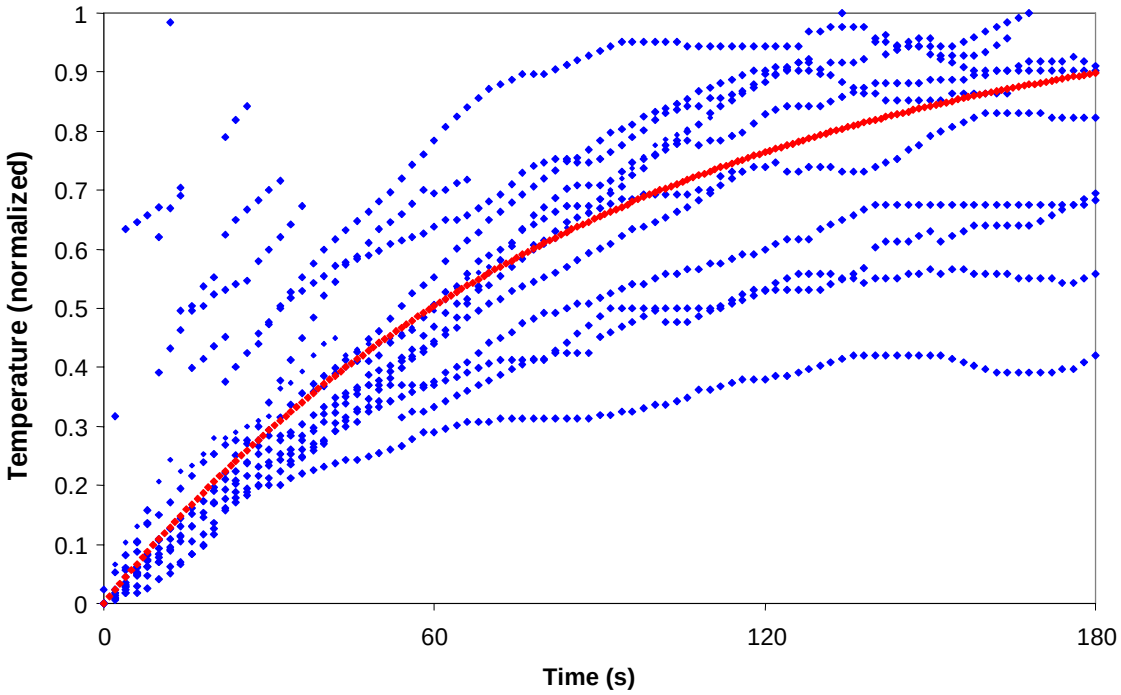

Figure A.1 – Normalized outside gear temperature response testing data with curve fit

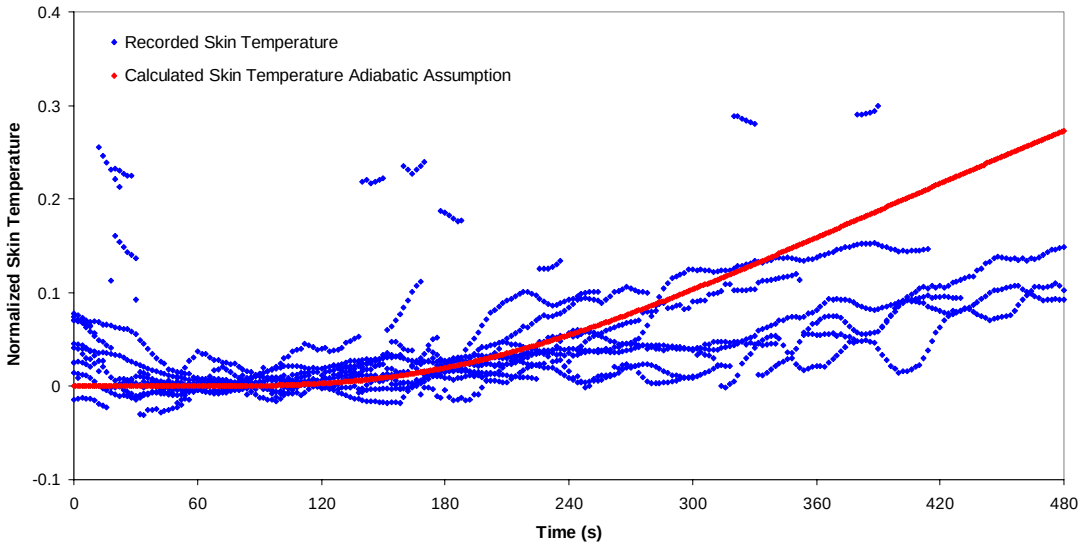

Figure A.2 – Compiled skin temperature responses for subjects wearing t-shirt, sweatshirt and gear including calculated curve fit

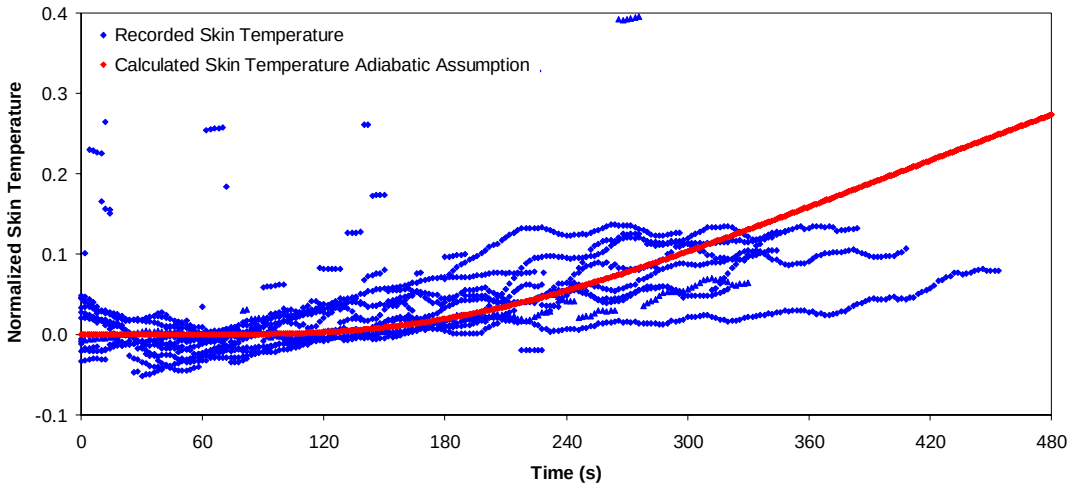

Figure A.3 – Compiled skin temperature responses for subjects wearing only a t-shirt and gear including calculated curve fit

Appendix B: MATLAB program source codes

Program 1: Single layer, fixed end temperatures

Boundary conditions:

T= 0	x=0
T= 1	x=l
T= 0	t=0

Governing equation:

$$Temp = \sum_{1}^{\infty} \frac{\sin\left(\frac{\pi \cdot n}{2}\right)}{\left(\frac{\pi \cdot n}{2}\right)} \left(1 - \exp\left(-\frac{\alpha \cdot n^2 \pi^2}{l^2} t\right)\right)$$

Program:

```
l=0.01;
alpha=4.5e-8;
PI = 3.1415926535897;

al2=alpha/l/l;

for t=1:1200

   time(t)=t;
   sum(t)=0;

   for n=1:50

      a=(sin(PI*n/2))/(PI*n/2);
      b=1-exp(-alpha*n*n*PI*PI/l/l*t);

      sum(t) = sum(t) + (a*b);

   end

end

  sum2=sum;

plot(time,sum2,'r.')
hold on
grid on
```

Program 2: Single layer, tri-diagonal, fixed alpha with fixed end temperatures

Boundary conditions:

T= 310 x=0
T= 450 x=*l*
T= 310 t=0

Governing equation:

$$-\frac{F_o}{2}\left(T_{n-1}^{N}\right)+\left(1+F_o\right)T_n^{N}-\frac{F_o}{2}\left(T_{n+1}^{N}\right)=T_n+\frac{F_o}{2}\left(T_{n+1}-2T_n+T_{n-1}\right)$$

Program:

```
dt= 2; %sec
dx=0.00005; %m

%%%%%%%%%%%%%%%%%%%%%%%%%
%asking for input parameters including # and type of layers
layers=input('How many layers are there, including skin? ')

disp('Choose the layers from the following list: ')

disp('Outer Shell:      1-Cotton Duck       2-Nomex III Defender    3-PBI Kevlar Kombat')
disp('Moisture Barrier: 4-Breathe-Tex       5-Breathe-Tex Plus      6-Nomex E-89
Crosstech      7-Neo-Guard     8-Nomex III Pajama Check')
disp('Thermal Liner:    9-Aralite')
disp('Other:            10-Scotchlite Trim      11-Skin      12-Cotton Shirt (Heavy)     13-
Cotton Shirt (Light)     14-50/50 Cotton Polyester Sweatshirt')
disp('                  15-Air GAp              16-Water')

layer(1)=input('Enter skin as the first layer: ')
for i=2:layers
layer(i)=input('What is the next layer: ')
end


%%%%%%%%%%%%%%%%%%%%%%%%%
%referencing property_list file and obtaining material properties

for i=1:layers
   [F(i),thickness,density(i),Cp(i),k(i)]=property_list(layer(i),dt,dx);     %referencing the
property_list file where the material properties are listed
   x(i)=round(thickness/dx);                                    %defining the number of
points per layer and rounding up to next interger

end
```

```
alpha=input('what is alpha: ')

xtotal = sum(x);              %defining total thickness of materials

kn(1)=k(1);               %W/mK
Cpn(1)=Cp(1);             %W-s/Kg C
densityn(1)=density(1);    %Kg/m^3


   for j=2:xtotal
   if j<=(x(1))
   alphan(j)=alpha;
   end

   if (j>(x(1)) && j<=(xtotal))
   alphan(j)=alpha;
   end

   Fnot(j)=alpha;
F1(j)=Fnot(j);
F2(j-1)=Fnot(j);

end

%%%%%%%%%%%%%%%%%%%%%%%%%%
%defining temps

for g=1:xtotal-1
    tempin(g)=310.;
end

temp_input1=450
%input('What is the room temperature (K)?')
temp_input2=300
%input('What is the outside (safe area) temperature (K)?')

tempin(xtotal)=temp_input1;        %defining outside temperature


%%%%%%%%%%%%%%%%%%%%%%
%defining a,b,c vectors

a(1)=0;
b(1)=1;
c(1)=0;
a(xtotal) = 0;
```

```
b(xtotal) = 1;
c(xtotal) = 0;

aold(1)=0;
bold(1)=1;
cold(1)=0;
aold(xtotal) = 0;
bold(xtotal) = 1;
cold(xtotal) = 0;


for n=2:xtotal-1
   a(n)=-F1(n)*dt/(2*dx*dx);
   b(n)=(1 + F1(n)*dt/(2*dx*dx)+F2(n)*dt/(2*dx*dx));
   c(n)=-F2(n)*dt/(2*dx*dx);

   aold(n)=F1(n)*dt/(2*dx*dx);
   bold(n)=(1 - F1(n)*dt/(2*dx*dx) - F2(n)*dt/(2*dx*dx));
   cold(n)=F2(n)*dt/(2*dx*dx);
end

%%%%%%%%%%%%%%%%%%%%
%defining initial r vector according to body temperature. all r values are
%the same to start because of the ramping function later on

for n=2:xtotal-1
   tempi(n)=310;
   r(n)= tempi(n)*aold(n)+bold(n)*tempi(n)+cold(n)*tempi(n);
end

%%%%%%%%%%%%%%%%%%%%
%defining times

total_time=600
%input('What is the total time duration (sec)?')
exit_time=600
%input('What time do you leave the room (sec)?')


%%%%%%%%%%%%%%%%%%%%%%%%%%%%%%%%
%defining iterations from times
total_iterations=total_time/dt;                %total number of iterations
exit_iterations=exit_time/dt;                  %exit time number of iterations

%%%%%%%%%%%%%%%%%%%%%%%%%%%%%%%%%%%%%%%%%%%%%%%%%%%%%%%%%%%%%%%%%%%%%%%
```

```
xaxis(1:xtotal)=1:xtotal;   %for graphing

r(1)=tempin(1);
for i=1:total_iterations

  r(xtotal) =temp_input1;
  tempout = trid(a,b,c,r);
  tempin=tempout;

  for n=2:xtotal-1
    r(n)=aold(n)*tempin(n-1)+bold(n)*tempin(n)+cold(n)*tempin(n+1);
    end

 tempout_norm=(tempout-310)/(temp_input1-310);

    skin=round(0.003/dx);
    pause(.1);

   subplot(1,2,1)
   plot(xaxis, tempout, 'kx')
   axis([0 600 300 450]);


%    subplot(1,2,2)
    hold on
    grid on
    axis([0 600 0 0.40]);
    plot(i*dt,tempout_norm(skin),'b.');
    title=('Temperature of skin');
    xlabel('Time (sec)');
    ylabel('Temperature (normalized)');

end

end
```

Program 3: Single layer, tri-diagonal, fixed alpha with outside ramping temperature

Boundary conditions:

T = 310 K x=0
T = f($Temp_{outsidegear}$) x=l
T = 310 K t=0

Governing equations:

$$-\frac{F_o}{2}\left(T_{n-1}^{N}\right)+\left(1+F_o\right)T_n^{N}-\frac{F_o}{2}\left(T_{n+1}^{N}\right)=T_n+\frac{F_o}{2}\left(T_{n+1}-2T_n+T_{n-1}\right)$$

$$Temp_{outside\ gear}=T_i-\left(T_i-T_{\max}\right)\cdot\exp\left(-\frac{t}{t_c}\right)$$

Program:

```
dt= 2; %sec
dx=0.00005; %m

%%%%%%%%%%%%%%%%%%%%%%%%
%asking for input parameters including # and type of layers
layers=input('How many layers are there, including skin? ')

disp('Choose the layers from the following list: ')
disp('Other:          11-Skin      18 - Defined thickness #1  19 - Defined thickness #2')


layer(1)=input('Enter skin as the first layer: ')
for i=2:layers
layer(i)=input('What is the next layer: ')
end

%%%%%%%%%%%%%%%%%%%%%%%%
%referencing property_list file and obtaining material properties

for i=1:layers
   [F(i),thickness,density(i),Cp(i),k(i)]=property_list(layer(i),dt,dx);     %referencing the
property_list file where the material properties are listed
   x(i)=round(thickness/dx);                                    %defining the number of
points per layer and rounding up to next interger

end

alpha=input('what is alpha: ')

%%%%%%%%%%%%%%%%%%%%%%%%
%setting the k, Cp, and density values per point
```

```
%calculating rhocpbar and F for each point
%so that the original Cp, k and density values are not disturbed, the new
%values are noted by the addition of an 'n', making kn, Cpn, densityn. The
%same for F, except it is called Fnot to calculate F1 and F2.

xtotal = sum(x);              %defining total thickness of materials

kn(1)=k(1);               %W/mK
Cpn(1)=Cp(1);              %W-s/Kg C
densityn(1)=density(1);     %Kg/m^3


   for j=2:xtotal
   if j<=(x(1))
   alphan(j)=0.0000000492;
   end

   if (j>(x(1)) && j<=(xtotal))       %
   alphan(j)=alpha;
   end

   Fnot(j)=alphan(j);
F1(j)=Fnot(j);
F2(j-1)=Fnot(j);

end

%%%%%%%%%%%%%%%%%%%%%%%%%%
%defining temps

for g=1:xtotal-1
    tempin(g)=310.;
end

temp_input1=450
%input('What is the room temperature (K)?')
temp_input2=310
%input('What is the outside (safe area) temperature (K)?')

tempin(xtotal)=temp_input1;        %defining outside temperature


%%%%%%%%%%%%%%%%%%%%%%
%defining a,b,c vectors

a(1)=0;
```

```
b(1)=1;
c(1)=0;
a(xtotal) = 0;
b(xtotal) = 1;
c(xtotal) = 0;

aold(1)=0;
bold(1)=1;
cold(1)=0;
aold(xtotal) = 0;
bold(xtotal) = 1;
cold(xtotal) = 0;
for n=2:xtotal-1
   a(n)=-F1(n)*dt/(2*dx*dx);
   b(n)=(1 + F1(n)*dt/(2*dx*dx)+F2(n)*dt/(2*dx*dx));
   c(n)=-F2(n)*dt/(2*dx*dx);

   aold(n)=F1(n)*dt/(2*dx*dx);
   bold(n)=(1 - F1(n)*dt/(2*dx*dx) - F2(n)*dt/(2*dx*dx));
   cold(n)=F2(n)*dt/(2*dx*dx);
end

%%%%%%%%%%%%%%%%%%%
%defining initial r vector according to body temperature. all r values are
%the same to start because of the ramping function later on

for n=2:xtotal-1
   tempi(n)=310;
   r(n)= tempi(n)*aold(n)+bold(n)*tempi(n)+cold(n)*tempi(n);
%tempin(n-1)*aold(n)+bold(n)*tempin(n)+cold(n)*tempin(n+1);
end

%%%%%%%%%%%%%%%%%%%%%
%defining times

total_time=600
%input('What is the total time duration (sec)?')
exit_time=600
%input('What time do you leave the room (sec)?')


%%%%%%%%%%%%%%%%%%%%%%%%%%%%%%%%%
%defining iterations from times
total_iterations=total_time/dt;                    %total number of iterations
exit_iterations=exit_time/dt;                      %exit time number of iterations
```

```
%%%%%%%%%%%%%%%%%%%%%%%%%%%%%%%%%%%%%%%%%%%%%

xaxis(1:xtotal)=1:xtotal;   %for graphing

r(1)=tempin(1);
for i=1:total_iterations

  r(xtotal) =temp_input1-(temp_input1-temp_input2)*exp(-0.011*i*dt);;
  tempout = trid(a,b,c,r);
  tempin=tempout;

  for n=2:xtotal-1
    r(n)=aold(n)*tempin(n-1)+bold(n)*tempin(n)+cold(n)*tempin(n+1);
    end

 temp_max=max(tempout);
 tempout_norm=(tempout-310)/(temp_input1-310);

    skin=round(0.003/dx);
    pause(.1);

figure(1)
    hold on
    grid on
    axis([0 600 0 0.70]);
    plot(i*dt,tempout_norm(skin),'c.');
    title=('Temperature of skin');
    xlabel('Time (sec)');
    ylabel('Temperature (normalized)');

figure(2)
  plot(xaxis, tempout, 'kx')
 axis([0 1000 300 450]);

end

end
```

Program 4: Multi-layer Program

Boundary conditions:

T = 310 K	x=0
T = f($Temp_{outsidegear}$)	x=l
T = 310 K	t=0

Governing equation:

$$-\frac{F_o}{2}\left(T_{n-1}^{N}\right)+\left(1+F_o\right)T_n^{N}-\frac{F_o}{2}\left(T_{n+1}^{N}\right)=T_n+\frac{F_o}{2}\left(T_{n+1}-2T_n+T_{n-1}\right)$$

$$Temp_{outside\ gear}=T_i-\left(T_i-T_{\max}\right)\cdot\exp\left(-\frac{t}{t_c}\right)$$

Program:

```
dt= 2; %sec
dx=0.00005; %m


%%%%%%%%%%%%%%%%%%%%%%%%%
%asking for input parameters including # and type of layers
layers=input('How many layers are there, including skin? ')

disp('Choose the layers from the following list: ')

disp('Outer Shell:      1-Cotton Duck       2-Nomex III Defender    3-PBI Kevlar Kombat')
disp('Moisture Barrier: 4-Breathe-Tex       5-Breathe-Tex Plus      6-Nomex E-89
Crosstech      7-Neo-Guard     8-Nomex III Pajama Check')
disp('Thermal Liner:    9-Aralite')
disp('Other:            10-Scotchlite Trim      11-Skin      12-Cotton Shirt (Heavy)     13-
Cotton Shirt (Light)     14-50/50 Cotton Polyester Sweatshirt')
disp('                  15-Air GAp              16-Water')

layer(1)=input('Enter skin as the first layer: ')
for i=2:layers
layer(i)=input('What is the next layer: ')
end


%%%%%%%%%%%%%%%%%%%%%%%%%
%referencing property_list file and obtaining material properties

for i=1:layers
   [F(i),thickness,density(i),Cp(i),k(i)]=property_list(layer(i),dt,dx);     %referencing the
property_list file where the material properties are listed
   x(i)=round(1*thickness/dx);                                    %defining the number of
points per layer and rounding up to next interger
```

```
end

%%%%%%%%%%%%%%%%%%%%%%%%%%%%%%%%
%defining points from the layers in order to assign dn, Cpn, densityn

y(1)=x(1);

for i=1:y(1)                % defining properties for first point
   kn(i)=k(1);              %W/mK
   Cpn(i)=Cp(1);              %W-s/Kg C
   densityn(i)=density(1);
end


for i=2:layers              % defining properties for all points, according to layer
   y(i)=x(i)+y(i-1);

   for j=(y(i-1)+1) : (y(i))
      kn(j)=k(i);           %W/mK
      Cpn(j)=Cp(i);           %W-s/Kg C
      densityn(j)=density(i);
   end

end

xtotal = sum(x);            %defining total thickness of materials including skin

for j=2:xtotal

   rhocpbar(j)=(densityn(j-1)*Cpn(j-1)+densityn(j)*Cpn(j))/2;
   rhocpbar(1)=rhocpbar(2);              %rhocpbar of the first point

   Fnot(j)=kn(j)/rhocpbar(j);
   F1(j)=Fnot(j);
   F2(j-1)=Fnot(j);
end


%%%%%%%%%%%%%%%%%%%%%%%%%%%%%%%%
%defining temps
tempin(1)=310;

for g=2:xtotal-1
    tempin(g)=310.;
end
```

```
temp_input1=500
%input('What is the room temperature (K)?')        %use if temp should be an input

temp_input2=300
%input('What is the outside (safe area) temperature (K)?')  %use if temp should be an
input

tempin(xtotal)=temp_input1;        %defining outside temperature


%%%%%%%%%%%%%%%%%%%%
%defining a,b,c vectors

a(1)=0;
b(1)=1;
c(1)=0;
a(xtotal) = 0;
b(xtotal) = 1;
c(xtotal) = 0;

aold(1)=0;
bold(1)=1;
cold(1)=0;
aold(xtotal) = 0;
bold(xtotal) = 1;
cold(xtotal) = 0;

for n=2:xtotal-1
   a(n)=-F1(n)*dt/(2*dx*dx);
   b(n)=(1 + F1(n)*dt/(2*dx*dx)+F2(n)*dt/(2*dx*dx));
   c(n)=-F2(n)*dt/(2*dx*dx);

   aold(n)=F1(n)*dt/(2*dx*dx);
   bold(n)=(1 - F1(n)*dt/(2*dx*dx) - F2(n)*dt/(2*dx*dx));
   cold(n)=F2(n)*dt/(2*dx*dx);
end


%%%%%%%%%%%%%%%%%%%%
%defining initial r vector according to body temperature. all r values are
%the same to start because of the ramping function later on

for n=2:xtotal-1
   tempi(n)=310;
   r(n)= tempi(n)*aold(n)+bold(n)*tempi(n)+cold(n)*tempi(n);
%tempin(n-1)*aold(n)+bold(n)*tempin(n)+cold(n)*tempin(n+1);
```

```
end

%defining times

total_time=600
%input('What is the total time duration (sec)?')
exit_time=600
%input('What time do you leave the room (sec)?')


%%%%%%%%%%%%%%%%%%%%%%%%%%%%%%%%%
%defining iterations from times
total_iterations=total_time/dt;                    %total number of iterations
exit_iterations=exit_time/dt;                      %exit time number of iterations


%%%%%%%%%%%%%%%%%%%%%%%%%%%%%%%%%%%%%%%%%%%%%%%%%%
%calculation. trid function refernce and ramping function

xaxis(1:xtotal)=1:xtotal;            %for graphing

r(1)=tempin(1);                      %initial r value

for i=1:total_iterations
  if i<exit_iterations

    r(xtotal) =temp_input1-(temp_input1-temp_input2)*exp(-0.011*i*dt);
    tempout = trid(a,b,c,r);
    tempin=tempout;

      for n=2:xtotal-1
          r(n)=aold(n)*tempin(n-1)+bold(n)*tempin(n)+cold(n)*tempin(n+1);
      end

      temp_max=max(tempout);
      tempout_norm=(tempout-310)/(temp_input1-310);
    end


  if i>exit_iterations
    r(xtotal) =temp_input2-(temp_input2-temp_max)*exp(-0.015*((i*dt)-
(exit_iterations*dt)+1));
    tempout = trid(a,b,c,r);
    tempin=tempout;

      for n=2:xtotal-1
```

```
        r(n)=aold(n)*tempin(n-1)+bold(n)*tempin(n)+cold(n)*tempin(n+1);
      end

      tempout_norm=(tempout-310)/(temp_input1-310);

  end
 %%%%%%%%%%%%%%%%%%%%%%%%
 %plots

  skin=round(0.003/dx);
  pause(.1);

  % normalized temperature of skin
  figure(1)
  hold on
  grid on
  axis([0 600 0 1]);
  plot(i*dt,tempout_norm(skin),'k.');

% Cross section figure
  figure (2)
  plot(xaxis, tempout, 'kx')
  axis([0 1200 290 500]);

%temperature of outside of gear
  Figure (3)
  hold on
  grid on
  axis([0 600 273 450]);
  plot(i*dt,tempout(xtotal),'b.');
  title=('Exterrior Gear Temperature');
  xlabel('Time (sec)');
  ylabel('Temperature (K)');

end
```

Program 5: Materials List

```
function [F,thickness,density,Cp,k] = property_list(layer,dt,dx)
switch layer

  case(1)
% Cotton Duck (Outer Shell)
thickness = 0.0013233 ; %m
density = 518.9   ; %Kg/m^3
Cp = 1620         ; %J/Kg °C     @50 °C
k = 0.1017        ; %W/m K       @55 °C

  case(2)
% Nomex III Defender (Outer shell)
thickness = 0.0008204 ; %m
density = 316.9   ; %Kg/m^3
Cp = 1510         ; %J/Kg °C     @50 °C
k = 0.0679        ; %W/m K       @55 °C

  case(3)
% PBI Kevlar Kombat (Outer Shell)
thickness = 0.0007976 ; %m
density = 321.8   ; %Kg/m^3
Cp = 890          ;%J/Kg °C      @50 °C
k = 0.073         ; %W/m K       @55 °C

  case(4)
% Breathe-Tex (Moisture Barrier)
thickness = 0.00122  ;  %m
density = 120.7  ;  %Kg/m^3
Cp = 2280         ; %J/Kg °C     @50 °C
k = 0.0441        ;  %W/m K      @55 °C

  case(5)
% Breathe-Tex Plus (Moisture Barrier)

thickness = 0.00111  ;  %m
density = 179.4   ; %Kg/m^3
Cp = 2050         ;  %J/Kg °C    @50 °C
k = 0.0461        ;  %W/m K      @55 °C

  case(6)
% Nomex E-89 Crosstech (Moisture Barrier)
thickness = 0.0009627 ; %m
density = 143.1   ; %Kg/m^3
Cp = 1900         ; %J/Kg °C     @50 °C
k = 0.0479        ; %W/m K       @55 °C
```

```
  case(7)
% Neo-Guard (Moisture Barrier)
thickness = 0.0005486  ;%m
density = 597.4    ;%Kg/m^3
Cp = 1480          ;%J/Kg °C     @50 °C
k = 0.1005         ;%W/m K      @55 °C

  case(8)
% Nomex III Pajama Check (Moisture Barrier)
thickness = 0.0005156 ; %m
density = 316.8   ; %Kg/m^3
Cp = 1930          ; %J/Kg °C     @50 °C
k = 0.0621         ; %W/m K      @55 °C

   case(9)
% Aralite (thermal liner)
thickness = 0.00359 ;   %m
density = 74.2  ;  %Kg/m^3
Cp = 1620          ; %J/Kg °C     @50 °C
k = 0.0462         ;%W/m K      @55 °C

  case(10)
% Scotchlite Trim (Trim)
thickness = 0.0007493 ; %m
density = 81.6   ; %Kg/m^3
Cp = 950          ; %J/Kg °C     @50 °C
k = 0.1269         ;%W/m K      @55 °C

  case(11)
% Skin
thickness = 0.0030   ;  %m
density = 1200      ; %Kg/m^3
Cp = 3558         ; %J/Kg °C     @50 °C
k = 0.21          ; %W/m K      @55 °C

case(12)
% Cotton Shirt (Heavy)
thickness = 0.00084   ;  %m
density = 317      ; %Kg/m^3
Cp = 1500         ; %J/Kg °C     @50 °C
k = 0.04          ; %W/m K      @55 °C

case(13)
% Cotton Shirt (light)
thickness = 0.00056   ;  %m
```

```
density = 316      ; %Kg/m^3
Cp = 1500          ; %J/Kg °C     @50 °C
k = 0.04           ; %W/m K       @55 °C

case(14)
% 50/50 Cotton Polyester Sweatshirt
thickness = 0.00130   ;  %m
density = 269      ; %Kg/m^2
Cp = 1600.         ; %J/Kg °C     @50 °C
k = 0.07           ; %W/m K       @55 °C

case(15)
% Air
thickness = 0.002   ;  %m
density = 1.13      ; %Kg/m^3
Cp = 1005          ; %J/Kg °C     @40 °C
k = 0.0271          ; %W/m K      @45 °C

case(16)
% Water
thickness = 0.0010   ;  %m
density = 980      ; %Kg/m^3
Cp = 4186          ; %J/Kg °C     @60 °C
k = 0.58           ; %W/m K       @65 °C

case(18)
% Defined thickness (only thickness is used)
thickness = 0.0050   ;  %m
density = 1200      ; %Kg/m^3
Cp = 3558          ; %J/Kg °C     @50 °C
k = 0.21           ; %W/m K       @55 °C

case(19)
% Defined thickness #2
thickness = 0.0124   ;  %m
density = 10      ; %Kg/m^3
Cp = 38          ; %J/Kg °C     @50 °C
k = 0.21           ; %W/m K       @55 °C


end

F=k/Cp/density*dt/(dx*dx);
```

Program 6: Tri-diagonal Function Solver

trid.m

```
%  Thomas algorithm for tridiagonal system

% | b_1 c_1                 | | fout_1 | = | fin_1 |
% | a_2 b_2 c_2             | | fout_2 | = | fin_2 |
% |     a_3 b_3 c_3         | | fout_3 | = | fin_3 |
% |       .   .   .         | |    .   | = |   .   |
% |           .   .   .     | |    .   | = |   .   |
% |               .   .   . | |    .   | = |   .   |
% |                 a_M b_M | | fout_M | = | fin_M |

% Note: x and y are dummy arrays
%       f array is overwritten by solution
%       a, b and c are preserved


function f = trid(a,b,c,f)
 m = length(f);
 x = zeros(m,1);
 y = zeros(m,1);

 %normalize the diagonal
 x(1)=c(1)/b(1);
 y(1)=f(1)/b(1);

 %forward sweep
 for i=2:(m-1)
    z=1/(b(i)-a(i)*x(i-1));
    x(i)=c(i)*z;
    y(i)=(f(i)-a(i)*y(i-1))*z;
 end

 y(m)= (f(m)-a(m)*y(m-1))/(b(m)-a(m)*x(m-1));

 %sweep backwards
 f(m)=y(m);

 for i=(m-1):-1:1
    f(i)=y(i)-x(i)*f(i+1);
 end
```

References

[1] William E. Mell and J. Randall Lawson. "A Heat Transfer Model for Fire Fighters' Protective Clothing." Technical Report NISTIR 6299. National Institute of Standards and Technology, Gaithersburg, MD, January 1999.

[2] K. Prasad, W. Twilley and J. Randall Lawson. "Thermal Performance of Fire Fighters' Protective Clothing. 1. Numerical Study of Transient Heat and Water Vapor Transfer." Technical Report NISTIR 6881. National Institute of Standards and Technology, Gaithersburg, MD August 2002.

[3] Scott Kukuck and Kuldeep Prasad. "Thermal Performance of Firefighters' Protective Clothing. 3. Simulating a TPP Test for Single-Layered Fabrics." Technical Report NISTIR 6993. National Institute of Standards and Technology, Gaithersburg, MD, January 2003.

[4] J. Randall Lawson and W. D. Walton. "Estimates of Thermal Properties for Fire Fighters' Protective Clothing Materials." Technical Report NISTIR 7282. National Institute of Standards and Technology, Gaithersburg, MD, June 2005.

[5] James Barry and Roger Hill. "Computational Modeling of Protective Clothing." Technical Report INJ. Creare Inc., 2003.

[6] Robert Vettori. "Estimates of Thermal Conductivity for Unconditioned and Conditioned Materials in Firefighters' Protective Clothing." Technical Report NISTIR 7279. National Institute of Standards and Technology, Gaithersburg, MD, November 2005.

[7] United States Fire Administration. (2002). *Firefighter Fatality Retrospective Study.* Emmitsburg, MD: Federal Emergency Management Agency.

[8] "Health and Safety Guidelines for Firefighter Training." University of Maryland, Center for Firefighter Safety Research and Development. Maryland Fire and Rescue Institute. College Park, MD. 2006. pp 118.

[9] Frank P. Incropera and David DeWitt. Fundamentals of Heat and Mass Transfer. John Wiley & Sons, Inc. 2002.

[10] National Fire Protection Association. The SFPE Handbook of Fire Protection Engineering. 2002.

[11] H. Carslaw and J. Jaeger. Conduction of Heat in Solids. Oxford at the Clarendon Press. 1959.

[12] Walfre Franco, Jorge Perez, Jie Liu, and Guillermo Aguilar. "Thermal Interaction of Cryogen Spray with Human Skin Under Vacuum Pressures." Department of Mechanical Engineering, University of California Riverside.

[13] T. Dai, B. Pikkula, L. Wang and B. Anvari. "Comparison of Human Skin Opto-Thermal Response to Near-Infrared and Visible Laser Irradiations: A Theoretical Investigation." Phys. Med. Biol. 49(2004) 4861-4877, October 8, 2004.

[14] Rahul Vallabh. "Thermal Barrier Properties of Flame Resistant Nonwovens." North Carolina State University. 2005.

[15] J. Randall Lawson and Tershia A. Pinder. "Estimates of Thermal Conductivity for Materials Used in Firefighters' Protective Clothing." Technical Report NISTIR 6512. National Institute of Standards and Technology, Gaithersburg, MD, May 2000.

[16] Teruo Kimura, Seiji Hatta, Satoshi Yamamoto, Kenzo Kadokura. "Thermal Conductivity of Substitute Lumbers Molded from Fiber Wastes." EcoDesign2003/2B-3. p. 331.

[17] M.N. Sun and K.P.S. Chen. "The Quality of Fabric Knitted from Cotton Sirospun Yarn." International Journal of Clothing Science and Technology, Vol. 12 No. 5, 2000, pp.351-359.

[18] Dupont. "Technical Guide for NOMEX Brand Fiber." H-52720. Revised July, 2001.

[19] Dupont. "Technical Guide for Kevlar Aramid Fiber." H-77848.

[20] M. Ziberna-Sujica and A. Pinteric. "Numerical Evaluation of Fabric Construction Parameters." International Journal of Clothing Science and Technology, Vol. 10 No.3/4, 1998, pp. 191-200.

[21] I. Frydrych, G. Dziworska, J. Bilska. "Comparative Analysis of the Thermal Insulation Properties of Fabrics Made of Natural and Man-Made Cellulose Fibres." Institute of Textile Architecture, Lodz, Poland. Fibers & Textiles in Eastern Europe. October/December 2002. pp 40-44.

[22] A. V. Popoola. "Dyeability of Cellulose Fibers Using Dyestuff from African Rosewood." Department of Industrial Chemistry, Federal University of Technology, Akure, Nigeria. Journal of Applied Polymer Science, Vol. 77, 746-751 (2000).

[23] Energy Saving Trust. "Insulation Materials Chart – Thermal Properties and Environmental Ratings." April 2004.